PART I SOLID-PHASE GROWTH OF GERMANIUM STRUCTURES

PART II CONDENSATION OF INJECTED ELECTRONS AND HOLES IN GERMANIUM

Thesis by

Vincent Marrello

In Partial Fulfillment of the

Requirements for the Degree of

Doctor of Philosophy

California Institute of Technology

Pasadena, California 91125

1975

(Submitted September 19, 1974)

Dedicata a miei genitori Alberto e Assunta e alla mia sposa Neneta

ACKNOWLEDGMENTS

It gives me great pleasure to express my deepest appreciation to Dr. James W. Mayer and Dr. Thomas C. McGill for their assistance, guidance, and encouragement thoughout the course of this work.

Aspects of this work reported here were performed in collaboration with Dr. J. O. McCaldin, M-A. Nicolet, G. Ottaviani, J. M. Caywood, R. N. Silver, I. L. Fowler and with Mr. T. F. Lee, T. A. McMath and R. B. Hammond. My sincere thanks to them all. Special thanks to Dr. C. A. Mead and K. Mathews for their assistance and insight.

I am also indebted to Dr. F. Eisen for the use and assistance with the 0.4 MeV accelerator at the North American Rockwell Science Center, Dr. I. L. Fowler for the use of the facilities at the Chalk River Nuclear Laboratories, Mr. J. R. Devany for scanning electron microscopy, Mr. A. A. Chodos for electron microprobe measurements, and Mr. H. Arnal for transmission electron microscopy and interpretation of diffraction patterns. My gratitude is extended to Dr. R. N. Hall and W. L. Hansen for supplying the high purity Ge crystals used during the course of this investigation. Thanks to Mr. R. Gorris for outstanding technical work, Mrs. P. Samazan for superb librarian work, and Mrs. K. Ellison and C. Norris for secretarial help.

I extend my gratitude to the U. S. Atomic Energy Commission, Office of Navel Research, Air Force Office of Scientific Research, IBM (Fellowship) and the Shlumberg Foundation (Fellowship) for their

financial support.

Most important I thank my wife, Neneta, for patiently typing my thesis.

ABSTRACT

PART I

Solid-solid reactions between a semiconductor and evaporated metal films can lead to semiconductor crystal growth. In this work, two aspects of solid-phase growth have been investigated; 1) growth of epitaxial Ge layers from a solid solution of Ge in an Al film onto single crystal Ge substrate (solid-phase epitaxy), and 2) growth of Ge crystallites in Al films from amorphous Ge films deposited on the Al film.

In solid-phase epitaxial studies, backscattering measurements with MeV $^{4}He^{+}$ ions showed that a solid-solid reaction occured at temperatures below the Ge/Al eutectic point. Channeling effect measurements with MeV $^{4}He^{+}$ ions indicated that the Ge layers were well-ordered and epitaxial. Electron microprobe measurements indicated the Ge layers contained Al. Hall effect measurements showed the Ge layers to be heavily p-doped. These Ge layers have been used to construct p-type contacts on p-n diodes, double injection diodes and nuclear particle detectors.

Ge crystallite growth in Al films occurs when an amorphous Ge film is deposited on an Al film and is heated at temperatures below the Ge/Al eutectic point. Crystallization of Ge occurs by an initial dissolution of Ge into the Al film followed by diffusion

and growth of Ge crystallites in the Al films.

The nature of Ge crystallite growth has been studied by MeV $^4He^+$ ion backscattering techniques, transmission electron diffractometry, scanning electron microscopy and electron microprobe analyis.

PART II

We demonstrate for the first time that the condensation of electrons and holes in Ge can be produced by electrical injection of carriers. The condensate occurs in double injection diodes at temperatures of at least up to 5°K.

The recombination radiation from the condensate was analysed using an infrared spectrometer. The LA- and TO-phonon assisted recombination radiation lines from the condensate occur at 709 meV and 700 meV respectively. The linewidth at half maximum of the 709 meV line is 3 meV. We measure a lifetime for the condensate of 40 μs. The radiation was emitted almost uniformly from the volume between the contacts of the double injection diode. The radiation intensity increased with increasing current and decreasing temperature.

LA-phonon assisted exciton and bound exciton recombination radiation lines at 714 meV and 712 meV respectively were observed from 7 to 15°K. Above 15°K, only the exciton line was observed. The recombination radiation lifetime of the exciton at 20°K is 6 μs.

Parts of this thesis have been previously published under the following titles:

Formation of Injecting and Blocking Contacts on High-Resistivity Germanium, G. Ottaviani, V. Marrello, J. W. Mayer, M-A. Nicolet, and J.M. Caywood, Appl. Phys. Lett., 20, 323 (1972).

Solid-Phase Epitaxial Growth of Ge Layers, V. Marrello, J. M. Caywood, J. W. Mayer, and M-A. Nicolet, Phys. Stat. Solidi, 13a 531 (1972).

High-Purity Germanium γ-Ray Spectrometers with Al Regrowth p^+ Contacts, V. Marrello, T. A. McMath, J. W. Mayer, and I. L. Fowler, Nuc. Instr. and Meth., 108, 93 (1973).

Crystal Growth of Silicon and Germanium in Metal Films, G. Ottaviani, D. Sigurd, V. Marrello, J. O. McCaldin, and J. W. Mayer, Science, 180, 948 (1973).

Crystallization of Evaporated Si/Ag and Ge/Al Films, D. Sigurd, G. Ottaviani, V. Marrello, J. W. Mayer and J. O. McCaldin, J. Non. Cryst. Solids, 12, 135 (1973).

Crystallization of Ge and Si in Metal Films I, G. Ottaviani, D. Sigurd, V. Marrello, J. W. Mayer and J. O. McCaldin, J. Appl. Phys., 45, 1730 (1974).

Condensation of Injected Electrons and Holes in Germanium, V. Marrello, T. F. Lee, R. N. Silver, T. C. McGill and J. W. Mayer, Phys. Rev. Lett., 31, 593 (1973).

Electron-Hole Condensate Radiation from Ge Double Injection Devices Between 1.5 and 4.2 K, V. Marrello, R. B. Hammond, R. N. Silver, T. C. McGill and J. W. Mayer, Phys. Lett., 47A, 237 (1974).

TABLE OF CONTENTS

PART I

SOLID-PHASE GROWTH OF Ge STRUCTURES

I. INTRODUCTION

A. General

Solid-solid reactions of various metal films with semiconductor surfaces have been shown to be very important to the operation, fabrication, performance and failure of modern electronic devices.[1-5] This has stimulated many independent investigations of the conditions and kinetics governing solid-solid reactions.[6-9] The results of these investigations have indicated that these reactions can occur rapidly at temperatures well below the eutectic point. For example, in a system exhibiting a simple eutectic behavior, such as Ge/Al,[10,11] Si/Al,[12,13] Si/Ag,[14] and Si/Au,[14,15] the semiconductor can dissolve at the interface and migrate into the metal film at temperatures below the eutectic point. Also in systems where compound phases exist, such as PdSi,[16] Ti-Al-Si,[17] and PtSi[18] formation of these compounds has been observed at low temperatures.

Crystal growth can occur from any nutrient medium: vapor, liquid, gel, or even solids.[19-22] Given that the appropriate conditions exist, solid-solid reactions can lead to crystal growth of a semiconductor on a single crystal substrate[13,23] or in the form of crystallites in a metal film.[24-26]

B. Epitaxial Growth of Ge Layers

A possible application of solid-solid reactions to crystal growth is shown schematically in Fig. 1. A metal film, in this case

Figure 1 Model for solid-phase epitaxial growth. a) Ge rapidly dissolves and diffuses into the Al film until the solubility limit, 2 atomic percent at 400°C, is reached. b) When the sample is cooled slowly to 250°C and held there, the solubility of Ge in the Al film drops to 0.2 atomic percent with the majority of the excess Ge growing onto the surface of the Ge substrate. The Ge layer incorporates Al while it is growing.

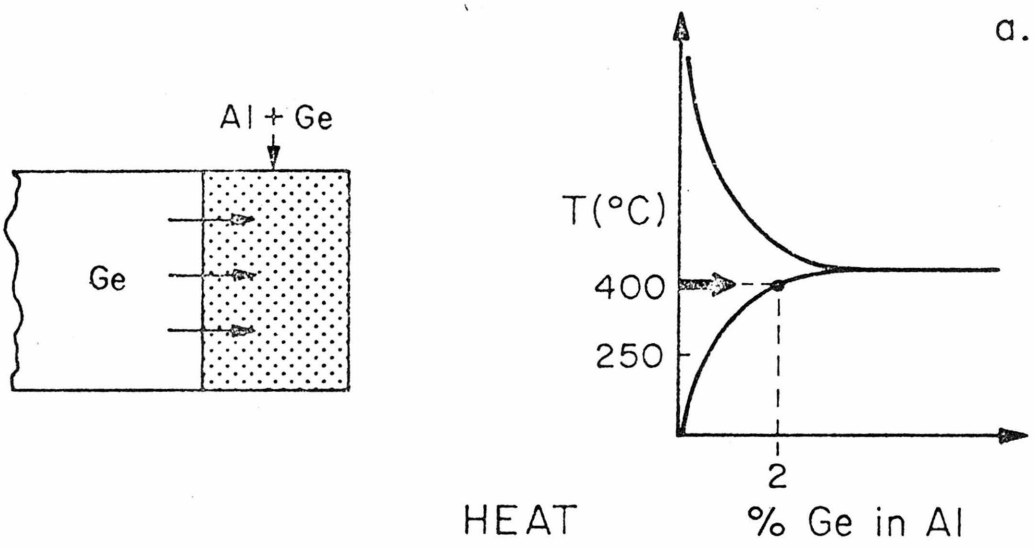
a.
Al + Ge
Ge
T(°C)
400
250
2
HEAT
% Ge in Al

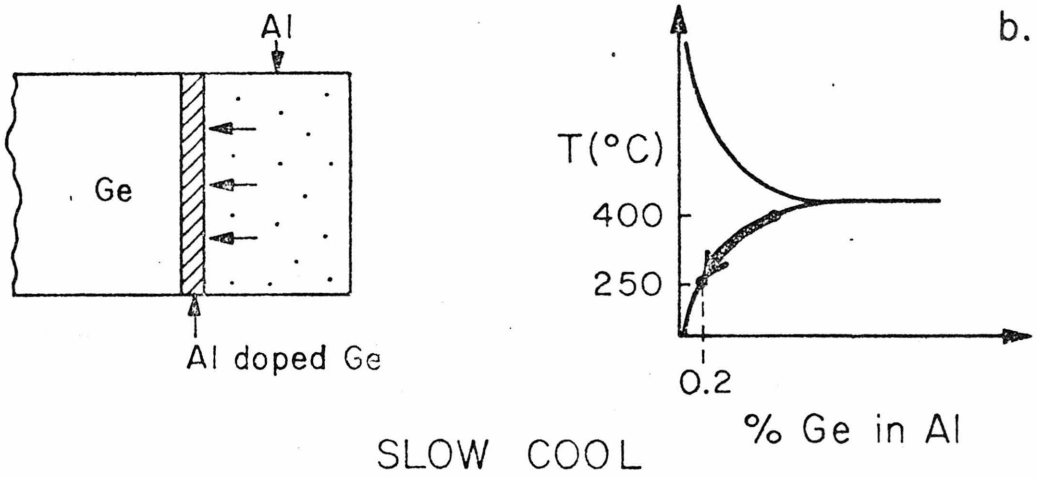
b.
Al
Ge
Al doped Ge
T(°C)
400
250
0.2
% Ge in Al
SLOW COOL

Figure 1

Al, is evaporated on a single crystal substrate, Ge. When the structure is heated to 400°C (a temperature below the eutectic point, 424°C[27]) Ge rapidly dissolves at the interface and diffuses into the Al film until the solubility limit is reached. Caywood[10] showed that the solubility of Ge in Al films was comparable to that in bulk Al and that it was reversible. When the structure is cooled slowly to 250°C, the solubility of the Ge in Al film drops, as indicated in Fig. 1. The amount of Ge in excess of the solubility can out-diffuse to the surface, precipitate in the Al film or grow onto the underlying crystal. In the case shown in Fig. 1 the majority of the excess Ge grew epitaxially on the surface of the single crystal Ge substrate.[23]

C. Ge Crystallite Growth

Although the Ge/Al system discussed above demonstrated solid-phase epitaxy, there are limitations on the thickness of Ge layer that could be grown due to the amount of Ge dissolved in the Al film. This difficulty can be overcome if an additional source of Ge is provided. One method would be to evaporate an amorphous Ge layer on top of the Al film.[26] The higher free energy of the amorphous state over the crystal state could provide a driving force for dissolution, transport and growth.[28]

Our results show that dissolution of the amorphous Ge layer, transport and crystal growth could take at constant temperature. However, rather than crystal growth onto the Ge single crystal substrate,

crystalline growth in the Al film took place. The details of this process and the data supporting these conclusions are presented in Section III.

D. Device Applications

Epitaxially grown semiconductor layers on crystal substrates have many techonologically important uses. Two of these uses are in the fabrication of Si intregated circuits[1] and GaAs laser diodes.[29] The conventional methods for growing epitaxial layers have been by liquid-phase epitaxy and vapour-phase epitaxy. These methods typically require temperatures of 800°C to 1200°C.[30,31]

Solid-phase epitaxial growth can occur at considerably lower temperatures and could potentially become very useful. Such growth has been demonstrated by our work in Ge[23] and by Sankur et al[13] in Si. The grown layer may be p-type or n-type depending in the metal film.

It has been demonstrated that for the Ge/Al system a heavily doped p-type epitaxial layer can result.[23] This layer has been used to form a hole-injecting contact for diodes,[32,33] transistors,[34] and double injection diodes.[32] The double injection diodes have been used down to liquid He temperatures in the study of electron-hole condensation in Ge discussed in Part II of this thesis. These layers have also been used as blocking contacts on nuclear particle detectors.[35]

Our studies reported in Section IV, were primarily aimed at showing that blocking and injecting contacts could be made by solid-phase growth in the Ge/Al system. To demonstrate blocking contacts, high resolution gamma detectors were fabricated in high purity Ge. To demonstrate injection, double injection diodes were built and evaluated.

II. SOLID PHASE EPITAXIAL GROWTH OF Ge LAYERS

In this section we describe our study of the dissolution and regrowth of Ge in Al films deposited on single crystal Ge substrates. The basic concepts are that the amount of Ge dissolved in the Al can follow a temperature cycle (i.e. is reversible) and that the excess Ge in the Al film can nucleate and grow at the Ge/Al interface. Electrical properties of the regrown layer should be determined by incorporation of the Al in the layer during growth.

A. Specimen Preparation and Analysis

Samples were prepared from 22 Ωcm, n-type Ge wafers with surfaces perpendicular to the (111) axis. One side of the wafers was lapped, polished with Mirrolux* and cleaned with organic solvents. The wafers were etched in $3HF:5HNO_3:3CH_3COOH$ for 15 s, quenched with deionized water, immersed in HF, washed with deionized water, dried with air and loaded into the evaporator. The system was then evacuated, and argon was leaked in to maintain a pressure at about 2×10^{-2} Torr against the diffusion pump. A plasma was then excited with a Tesla coil for ~ 20 s, the argon flow was cut off, and an Al film was evaporated on the polished surface of the wafers. Next, samples were heated in a tube furnace at 390 to 400 °C for 30 min, slow cooled

*Registered trademark of Materials Development Corporation, Los Angeles, California.

(~ 3°C/min) to 250°C and held there for 60 min. The furnace was opened, allowing the samples to cool quickly to room temperature (~ 15°C/min).

Hall patterns were electrically isolated from the substrate by mesa etching in $3HF:3HNO_3:5CH_3COOH$ for 30 s. Black wax was used to protect the four contact pads and the Al film was then removed with an Al etchant.* X-ray flourescence with an electron microprobe was used to interpret contrast in the scanning electron micrographs. Scanning electron micrographs showed that the Al film had been etched away completely. After removal of the Al film, the layers grown on the wafers were electrically evaluated using the van der Pauw method for measuring sheet resistivity and Hall voltage. Similar techniques have been used for evaluating ion implanted layers.(36)

The channeling spectra were measured using 0.4 and 2.0 MeV $^4He^+$ ion beams. The specimens were mounted on a two-axis goniometer. Back-scattered particles were detected by a surface barrier detector set at an angle of 164° to the direction of the incident beam. The energy resolution of the system was equivalent to a depth resolution of ~ 200 Å. At 2 MeV, the depth which could be probed to determine lattice structure was ~ 8000 Å. The amount of Al in the grown layer was measured with an electron microprobe at 10 kV. With this accelerating potential, the probe has a sampling depth of ~ 3000 Å and a sensitivity

*Transene Corp., Browley, Massachusetts.

to Al dissolved in Ge of better than 0.2 atomic percent.

B. Results

Hall voltage polarities and hot point probe measurements on the grown Ge layer indicated hole conductivity. Typical samples on which 10 μm of Al had originally been deposited conducted ~ 20 mA from contact to contact (6 mm) with 0.5 V applied, independent of temperature from 170 to 300 °K. The ratio of this sheet current in the grown layer to the leakage current into the substrate was high enough to distinguish between contributions from the grown layer and from the substrate. For example, these same samples typically showed contact to substrate leakage current of 0.5 mA at 300°K and less than 1 μA at 170°K under 0.5V reverse bias. Previous measurements [36] of ion-implanted layers indicated that electrical properties of doped layers could be accurately evaluated if the leakage current was less than 5% of the sheet current. Our samples met this criterion.

The sheet resistivity, ρ_s, and Hall mobility, μ_H, were measured on layers produced with deposited Al films of various thicknesses. All samples were processed in the same way. Measurements at 285 and 170°K yielded $\rho_s = 25.5\,\Omega/\square$, $\mu_H = 15$ cm^2/Vs and $\rho_s = 22.2\,\Omega/\square$, $\mu_H = 17$ cm^2/Vs, respectively, for a grown layer sample which had 11 μm of deposited Al. This measured Hall mobility is in good agreement with reported measurements on heavily doped Ge crystals.[37] Assuming that Hall mobility is the same as drift mobility,[38] the number of acceptors

per unit area is 1.6×10^{16} /cm^2. For this same sample, the Al concentration in the grown Ge layer, measured by X-ray fluorescence gave a value of 0.5 atomic percent. This is equivalent to $\sim 10^{16}$ Al atoms/cm^2 over 3000 A.

Hall measurements of a Ge layer grown on a sample which had originally 9 μm of deposited Al, but heated for 160 min at 400°C gave a value of $N_s = 1.2 \times 10^{16}/cm^2$. This is essentially the same as that obtained after the standard 30 min treatment. However, a grown layer prepared from a thinner (6.6μm) Al film yielded a significantly smaller value, $N_s = 2.5 \times 10^{15}/cm^2$. Channeling effect measurements were made on a grown Ge layer prepared from an 11 μm thick Al film. Rotational scans around the (111) axis of the substrate indicated that the grown layer has the same axis of orientation and the same three-fold planar symmetry as the crystal substrate. Figure 2 shows random and (111) aligned spectra of backscattered 0.4 MeV ^{4}He particles. The ratio of aligned to random yields just behind the surface peak (in the vicinity of 300 keV), called the minimum yield, is $\sim$ 5% indicating that the regrown layer is well ordered. In measurements at 0.4 and 2.0 MeV no discontinuities were noted in the aligned yield, indicating the absence of gross lattice disorder at the interface between grown layer and substrate.

Backscattering measurements with 2 MeV $^4He^+$ ions were made to show that alloying (liquid phase formation) does not occur for heat treatments below the eutectic temperature. For this purpose, thinner

Figure 2 Random (circles) and (111) aligned (dots) spectra of backscattered 0.4 MeV $^{4}He^{+}$ ions from sample with a Ge layer prepared from an 11 μm Al film. The Al film had been removed after heat treatment. Note that the vertical scale for the aligned spectrum is magnified three times.

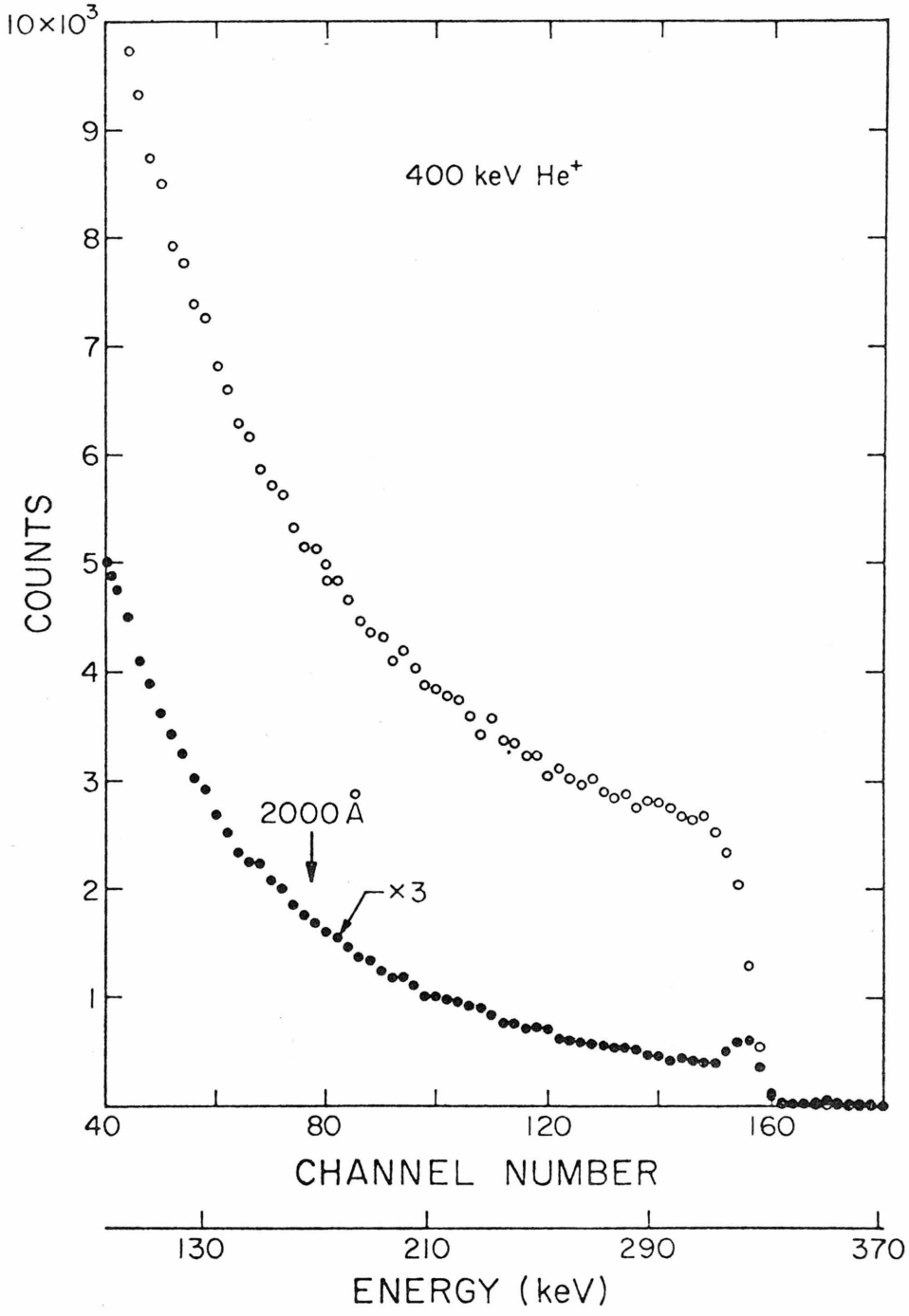
10×10³
9
8
7
6
5
4
3
2
1
COUNTS
400 keV He⁺
2000 Å
×3
40
80
120
160
CHANNEL NUMBER
130
210
290
370
ENERGY (keV)

Figure 2

Al layers (~ 2000 Å) were used so that the backscattering yield from both the Al and Ge could be detected. The spectrum shown in Fig. 3a is for a sample heated to 395°C (i.e. below the Al/Ge eutectic at 424°C) and quenched. The signal from Al (shaded area) has a well defined line shape indicating that the layer is uniform. The signal from the Ge substrate is shifted to lower energy due to the presence of the overlaying Al layer. Backscattering events from Ge atoms in the Al layer give rise to a "foot" in the spectrum extending out to the Ge edge. (The Ge edge corresponds to the energy of particles scattered from Ge atoms located at the sample's surface). The shape of the "foot" indicates that the Ge is uniformly distributed within the Al layer, as had been found in the previous investigation of the solubility of Ge in Al films.[10]

The properties of a Ge/Al structure heated above the eutectic temperature where alloying is expected to occur are markedly different; there is even a change in the visual appearance of the surface. Figure 3b is the backscattering spectrum for a sample heated at 430°C; the Al signal (shaded portion) is not well defined and the signal from the Ge substrate is shifted to the Ge edge. The dashed line represents a portion of the spectrum of a virgin Ge sample; the crosshatched portion indicates that a Ge sample heated above the eutectic contains a substantial concentration of Al dissolved in the Ge. The forward shift in the Ge signal to the position of the Ge edge and the decrease in the Al signal are characteristic of an alloyed sample. Similar features were

Figure 3 Energy spectra of 2 MeV $^4He^+$ ions backscattered from Ge samples with ~ 2000 Å Al films following anneal at a) 395°C and b) 430°C. The arrows indicating the positions of the Al and Ge edge correspond to energies of particles scattered from Al and Ge at the sample surface.

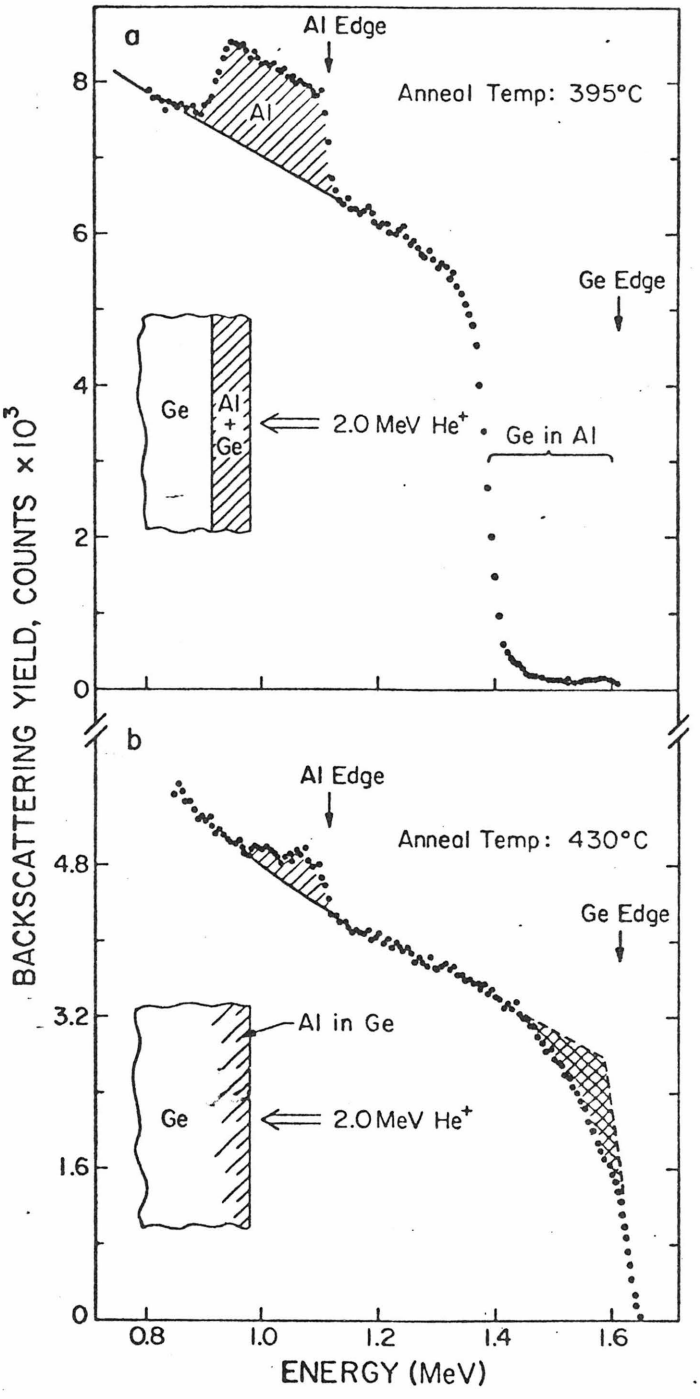
a
Al Edge
Anneal Temp: 395°C
Al
Ge Edge
Ge
Al + Ge
2.0 MeV He+
Ge in Al
b
Al Edge
Anneal Temp: 430°C
Ge Edge
Al in Ge
Ge
2.0 MeV He+
BACKSCATTERING YIELD, COUNTS ×10^3
ENERGY (MeV)
0
2
4
6
8
1.6
3.2
4.8
0.8
1.0
1.2
1.4
1.6

Figure 3

found in an investigation of the alloying behavior of Au layers on GaAs.[5]

C. Discussion and Conclusion

Comparison of the spectra in Fig. 3a and b confirms that alloying processes are not responsible for the p-type behavior observed in the Ge/Al structures. When the samples are heated to 400°C, Ge dissolves and diffuses into the Al (Fig. 3a) until the solubility limit at 400°C (~ 2 atomic percent) is reached.[10,27] When the sample is cooled slowly, the concentration of the Ge in the Al film drops to the equilibrium concentration at 250°C (0.2 atomic percent) with the majority of the excess Ge growing on the surface of the Ge substrate. For an 11 μm Al film, one calculates from the Ge solubility in Al that the thickness of a uniform grown layer would be 2700 Å. Thermodynamic considerations indicate that the regrown Ge layer should incorporate Al to the solubility limit at the growth temperature, approximately 0.6 atomic percent. One therefore estimates the number of Al atoms to be approximately 1×10^{16} /cm^2 for a sample with a 11 μm Al layer, in good agreement with electrical masurements ($N_s = 1.6 \times 10^{16}$ /cm^2) and electron microprobe measurements.

During heat treatment at 400 °C diffusion of Al into the Ge crystal is expected to proceed very slowly. The reported[40] diffusion coefficient of Al in Ge is 1×10^{-15} cm^2/s at 670°C and 2×10^{-12} cm^2/s at 900°C. The extrapolated diffusion coefficient at 400°C is less than

10^{-21} cm^2/s. This latter value implies that in 30 min less than 10^{12} Al atoms/cm^2 diffuse into the Ge substrate at 400°C; a value which is three to four orders of magnitude less than the hole concentration observed in our Hall measurements. Further, the number of holes in the layer does not depend on process at 400°C, contrary to the behavior expected from diffusion theory. Consequently, diffusion of Al into the Ge substrate probably is not a dominant contribution to the measured value of N_s.

The epitaxial growth predicts that N_s should vary with the thickness of the Al layer, but not with time at fixed process temperature (as long as the times are long enough to allow the Ge to reach solubility limits in the solvent, Al). Experimental results agree with this model as the measured values of N_s increase with increasing Al film thickness and are independent of time at 400°C.

Channeling results indicate that growth from the Al films is epitaxial with the Ge substrate. The minimum yield values, 5%, are only slightly higher than the 4% value for the (111) axis in single crystals.[41]

In summary we have shown that solid Al films can serve as a solid solvent from which dissolved Ge may grow epitaxially on a Ge substrate. The resultant Ge layer is heavily p-doped and has a Hall mobility for holes in agreement with that reported for heavily doped bulk Ge crystals.

III. GROWTH OF Ge CRYSTALLITES IN Al FILMS

In this section we consider an alternative approach to the one used in Section II. Here, an amorphous Ge film and an Al film are sequentially deposited on a single crystal substrate. During heat treatment, dissolution of the amorphous Ge should provide a source for growth of a single crystal Ge layer onto the underlying single crystal substrate. This method offers the advantage of growing Ge layers whose thickness depends on the amount of Ge evaporated.

In this work, we were primarily interested in the dissolution and transport of the amorphous Ge and not in epitaxial growth on the substrate. All heat treatments were carried out at temperatures below the Ge/Al eutectic (424 C).

A. Specimen Preparation and Analysis

Specimens for this investigation were prepared by vacuum deposition of Al and Ge onto substrates of Ge, Si and in a few cases vitreous carbon. One side of the Ge wafer was polished, and the following procedure was used to clean the surface before evaporation. The wafers were etched in $3HNO_3$:1HF for ~ 30 s and afterwards quenched in deionized water. Then the samples were immersed in dilute solution of HF and removed just before loading into the evaporation chamber. The geometry of the system is such that the samples, held at room temperature, are mounted ~ 20 cm above the source. A quartz-oscillator thickness monitor

is located at roughly the same height. For all elements used, the rate of deposition were 10 to 40 A/s as monitored by the quartz oscillator. These evaporation conditions have been shown to produce amorphous layers of Ge.[42,43] This was confirmed for our films by transmission electron diffraction. Immediately after unloading the evaporation system, the samples were heat treated in a quartz tube furnace with dry N_2 atmosphere. After heat treatment, samples were quenched by pulling them out of the furnace.

Two sequences of evaporation were used: either substrate/metal/semiconductor or substrate/semiconductor/metal. The range of thicknesses were between 3000 and 5000 Å for Al and 50 to 2000 Å for Ge. The actual thicknesses of the films were measured by backscattering of MeV $^4He^+$ ions.[44] This technique gives thickness values in atoms/cm^2. For convenience, we assume bulk density and give thicknesses in angstroms. The samples were studied by four different techniques: MeV $^4He^+$ ion backscattering, scanning electron microscopy and electron microprobe analysis.

Backscattering measurements give the distribution of elements as a function of depth within the sample.[44] To obtain the lateral distribution, scanning electron microscopy and electron microprobe analysis were used. To obtain cross-sectional views of the structures, samples were cleaved in liquid nitrogen to avoid smearing of the metal. For scanning electron microscopy, etching and cleaning of the samples were required in some cases. The Al was etched by dilute

NaOH. For electron microprobe studies of the lateral distribution of the semiconductor in the metal film, it is necessary to avoid interference from the underlying substrate. For the films studied in this work, some contribution from the Ge substrate was found even at the lowest electron energy used (4 keV). The substrate interference could be eliminated by using C or Si substrates for the Ge/Al films.

B. Results and Discussion

During heat treatment at 100 to 300°C, Ge moves into the Al film. This is evident from the backscattering spectra shown in Fig. 4, for two samples annealed at 300°C. The component due to Ge atoms in the composite film appears in the energy region of 1.4 to 1.6 MeV, the region between the shoulder of the Ge thick target yield and the energy position corresponding to Ge atoms at the surface (indicated by the arrow). The two samples had different thicknesses of evaporated Ge, 130 Å and 220 Å respectively, as measured on Ge films deposited simultaneously on Si samples. This difference in the quantity of evaporated Ge is reflected in the heights of the plateaus due to the Ge in the composite film. Within the accuracy of the backscattering measurements all the evaporated Ge moves into the Al film. In Fig. 4, the edges of the Al signal are sharp, indicating that the composite structure is uniformly thick over the ~ 2 mm^2 area probed by the analyzing $^4He^+$ beam.

Figure 4 2 MeV $^{4}He^{+}$ spectra from Ge/Al structures annealed at 300 °C. The squares indicate portion of the samples covered by Al but not with Ge.

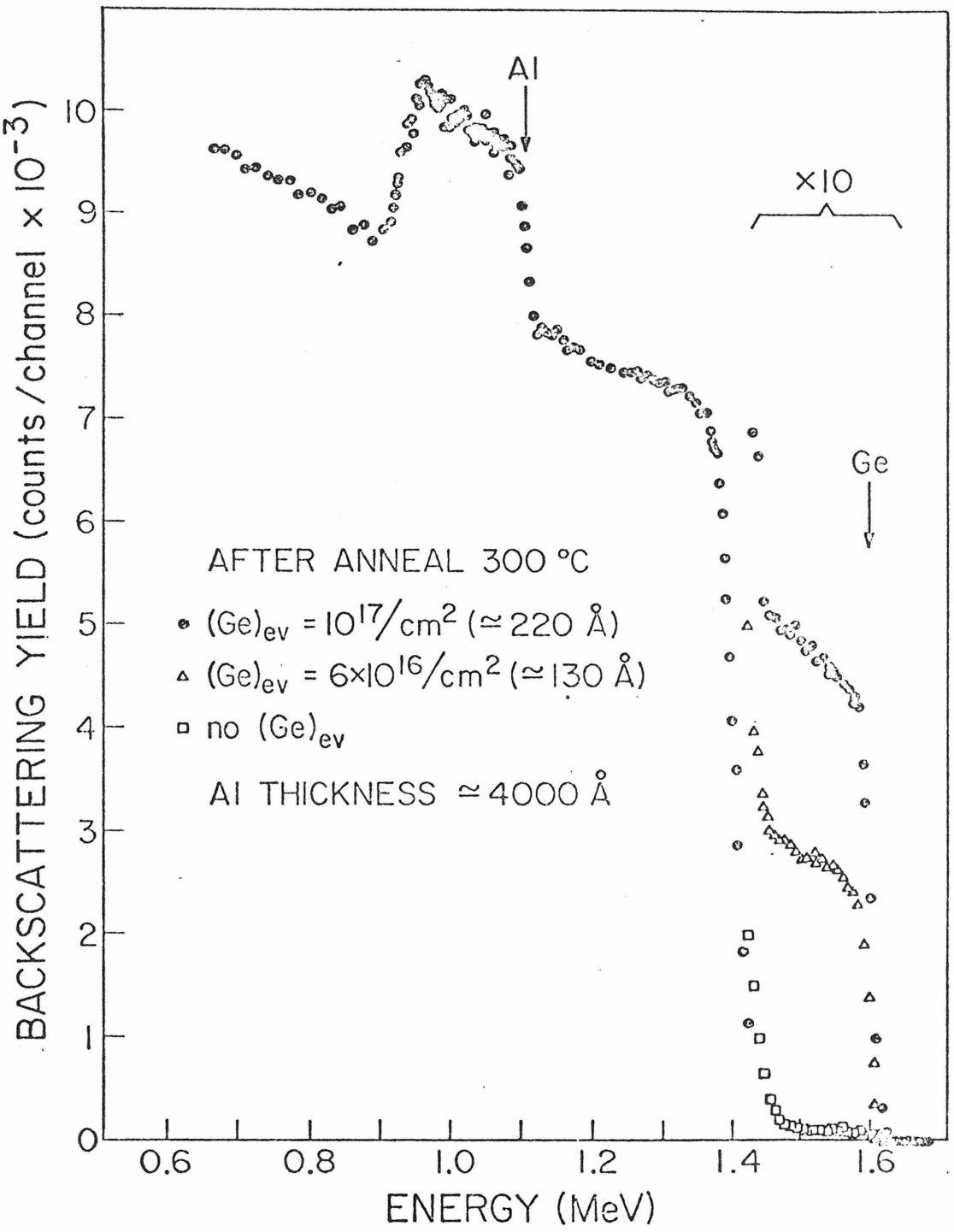
BACKSCATTERING YIELD (counts/channel x 10^{-3})
ENERGY (MeV)
Al
Ge
×10
AFTER ANNEAL 300 °C
$(Ge)_{ev} = 10^{17}/cm^2$ (≃ 220 Å)
$(Ge)_{ev} = 6\times10^{16}/cm^2$ (≃ 130 Å)
no $(Ge)_{ev}$
Al THICKNESS ≃ 4000 Å
0
1
2
3
4
5
6
7
8
9
10
0.6
0.8
1.0
1.2
1.4
1.6

Figure 4

were masked so that a portion of the sample had only an evaporated layer of Al. In this portion of the sample, Ge from the single crystal substrate is dissolved into the Al film as indicated by the lowest data points (squares). In this case, however, the amount of Ge in the Al is determined by the solid solubility and is ~ .5 atomic percent at 300°C.[10,39]

The motion of Ge into the Al film can be seen more clearly when Si substrates are used. Figure 5a shows the backscattering spectrum for a 100 Å Ge layer covered with a 4000 Å Al film. After the sample was heated at 100°C for 140 min , some of the underlying Ge has moved into the Al film (Fig. 5b). After 350 min, the Ge is distributed in depth throughout the composite film structure (Fig. 5c).

Figure 5 shows that the Ge distribution changes with successive heat treatments. These results as well as those obtained by scanning electron microscopy, as indicated below, clearly show that the Ge/Al intermixing predominantly occurs during heat treatment and not during cooling.

The amount of Ge contained in the composite films after anneal, as measured by backscattering, was orders of magnitude above the solid solubility of Ge in Al. The results of scanning electron micrographs of the surface show that at the surface there are localized regions of Ge in a surrounding Al matrix. Further information was obtained from electron microprobe analysis which showed that the Ge was in the form of precipitates with lateral sizes of 2000 to 40,000 Å.

Figure 5 Spectrum for a 100 Å Ge layer covered by a 4000 Å Al layer on a Si substrate. The arrows show the energy positions for Al and Ge at the surface. The backscattering component from the Si substrate is not visible because components below 1.0 MeV are suppressed.

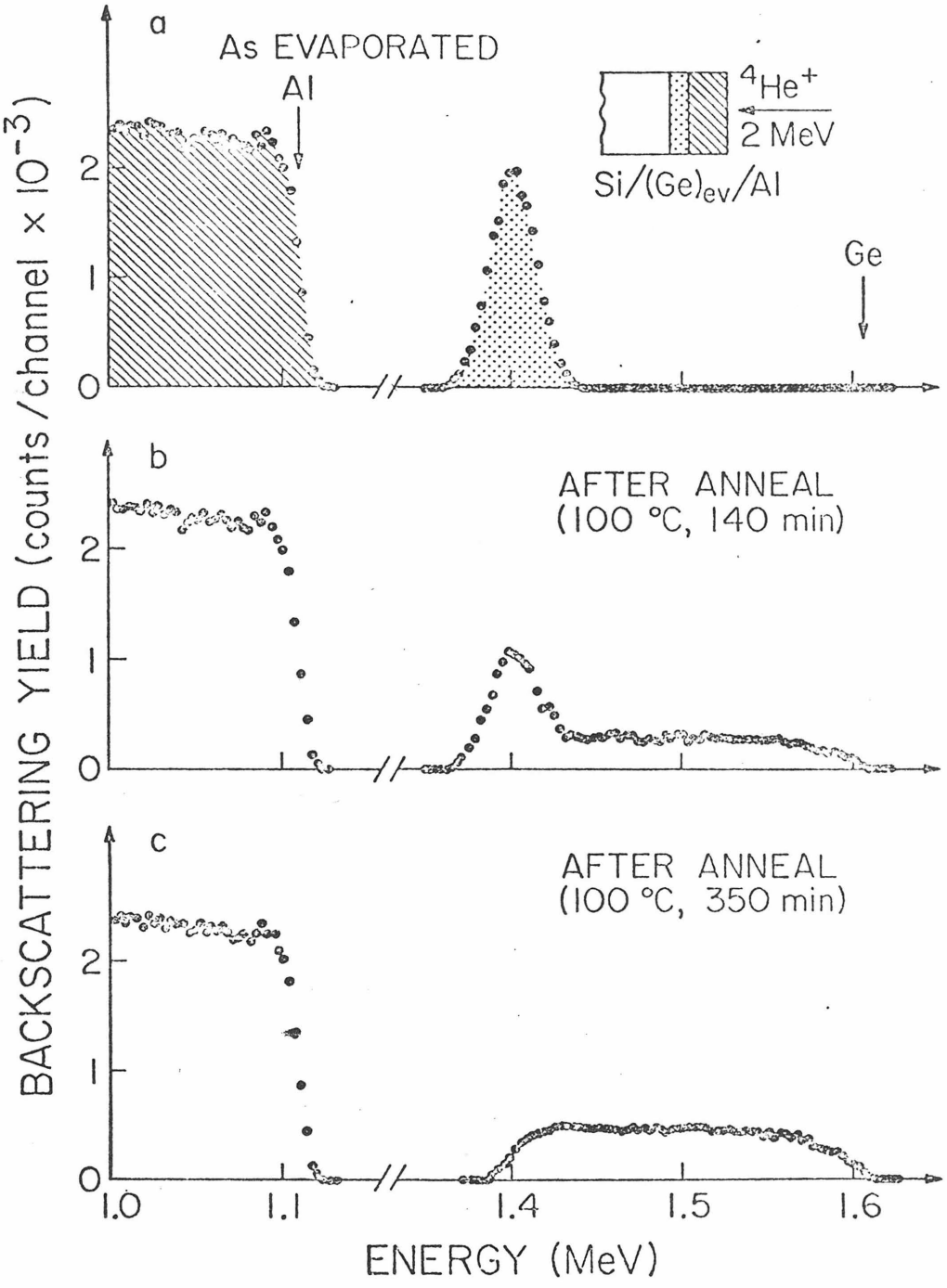
a
As EVAPORATED
Al
$^4He^+$
2 MeV
Si/(Ge)$_{ev}$/Al
Ge
b
AFTER ANNEAL
(100 °C, 140 min)
c
AFTER ANNEAL
(100 °C, 350 min)
BACKSCATTERING YIELD (counts /channel × 10^{-3})
0
1
2
1.0
1.1
1.4
1.5
1.6
ENERGY (MeV)

Figure 5

Scanning electron microscopy techniques were also used to examine the Ge precipitates on cleaved and on etched samples. Figure 6 shows micrographs of a sample with 1840 Å of Ge and 3600 Å of Al after heating at 300°C for 60 min. The upper micrograph (Fig. 6a) of a cleaved surface shows Ge precipitates (appearing as white islands) imbedded in a matrix of Al. The top surface of the composite film is relatively flat. This same sample was etched to remove the Al. The Ge precipitates (Fig. 6b) are smooth topped with some indication of undercutting near the Si substrate. This undercutting can be seen more clearly in Fig. 6c which is a micrograph taken at a greater angle of incidence to the surface. Portions of the film were stripped off the substrate after heat treatment and were studied in a transmission microscope. Electron diffraction patterns clearly showed that the precipitates were crystalline in nature.[24]

C. Conclusions

We have studied the behavior of amorphous Ge in contact with metal layers. The Ge/Al case was chosen as representative of a simple eutectic system. A wide range of experimental techniques were used: scanning electron microscopy, MeV $^4He^+$ ion backscattering, electron microprobe and transmission electron diffraction. Taken together, experimental data utilizing these techniques lead to a consistent description.

Of the many reaction paths one can imagine to carry the amorphous

Figure 6 Scanning electron micrographs at 10 keV electron energy of a Si substrate covered by 1840 Å Ge and 3600 Å Al and annealed at 300°C for 1 hour. (a) shows a cleaved surface taken with the electron beam incident at 80° off the surface normal. (b) and (c) shows the sample after removing the Al. In these cases the electron beam was incident at 65° and 85° respectively.

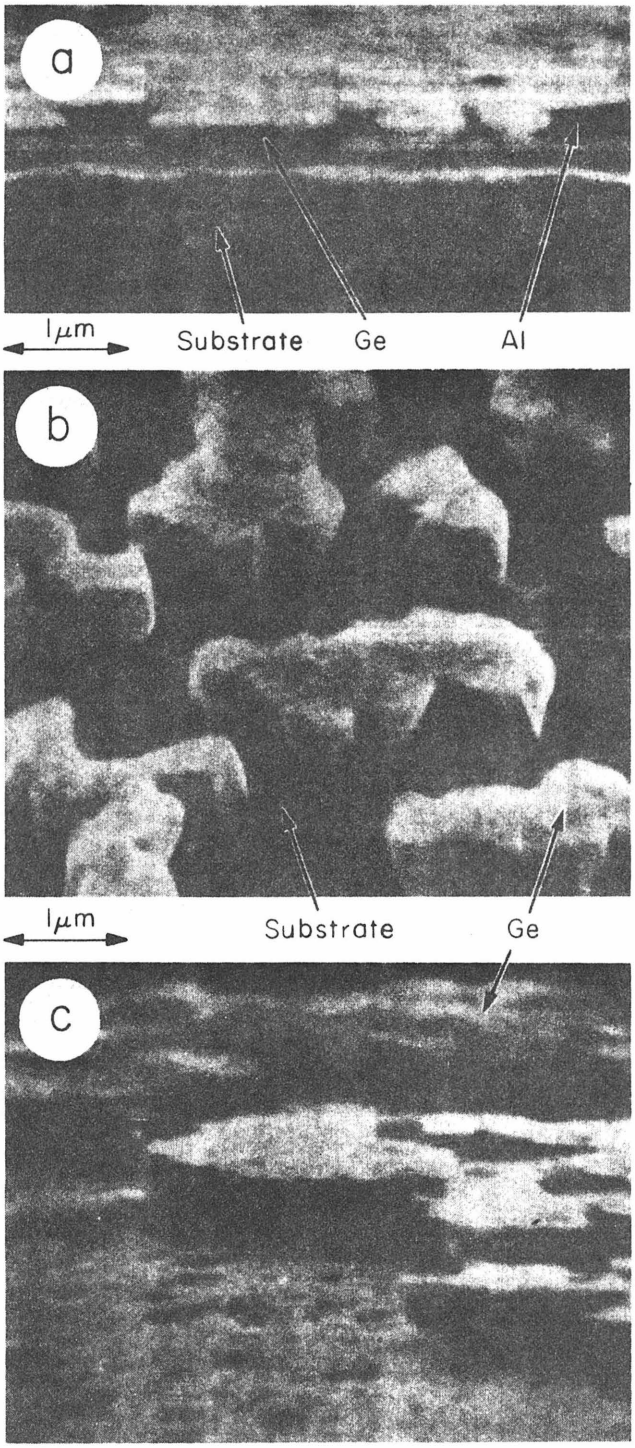

Figure 6

semiconductor into its lowest energy, e.g. crystalline state, we find a particularly simple path to be operative in the systems we have investigated. This path consists of dissolution of the amorphous Ge into the adjacent solid metal film and growth of crystallites from solution out of the metal.

Energetically, the driving force for this isothermal dissolution and crystallite growth is provided by the higher free energy of the amorphous material as compared to the crystalline material. Kinetically, the metal layer provides the necessary solvent medium for the easy reaction path just described.

Subsequent investigations by Canali et al[45] indicated that the interface between the Al film and the single crystal Ge substrate was crucial for epitaxial growth. The interface had to be free of any oxide layer or other contaminants to provide a clean surface for nucleation. Under these conditions, they were able to demonstrate solid-phase epitaxial growth on Ge substrates from an amorphous Ge layer deposited on an Al film.

IV. DEVICE APPLICATIONS OF SOLID-PHASE EPITAXIAL GROWTH OF Ge LAYERS

A. Germanium Nuclear Particle Detectors

In Section II it was shown that p-type layers of Ge could be grown epitaxially on single crystal Ge substrates. The objective of this study was to determine if high-quality, large area, blocking contacts could be formed. The performance of reversed-biased nuclear detectors has been shown to depend critically on the blocking nature of the contacts. Consequently, high-purity Ge γ-ray detectors were fabricated using regrowth techniques to test the blocking quality of the contact[35]. The facilities of Chalk River Nuclear Laboratories were used in this cooperative program.

1. Detector Fabrication

After the sample had been cut to shape, it was etched for one min in a $3HNO_3$:1HF solution. Lithium was evaporated onto one face and diffused for five min at 300°C. The opposite face was lapped with 5 μm alumina slurry and given a final "Mirrolux" polish. The sample was then degreased and lightly etched again (30 s to 60 s in $3HNO_3$:1HF), rinsed throughly with water, and immersed in HF. Immediately before placing the sample in the evaporator, it was rinsed again with water and blown dry with a nitrogen gas jet. A layer of aluminum 1000 to 4000 Å thick was evaporated onto the cleaned face, with a bell jar pressure of ~ 10^{-6} Torr. A bias of +1000 V was placed

on the tungsten filament with respect to the sample during evaporation. After evaporation the sample was placed in an oven with argon flow through it, heated to 300°C for twenty min, then cooled slowly (~ 2 to 3°C/min). The lithium contact was lightly lapped, then both contacts are masked, and the detector was given a final etch (two min in $3HNO_3$:1HF). Electronic grade chemicals and double distilled water were used at all stages.

2. Results

On the basis of previous experience with Ge lithium-drift and high purity Ge detectors evaluated on normal electronic systems, leakage currents less than 1 nA are required for good energy resolution.(46) Detectors on p-type high purity material have been made using Al/Ge regrowth technique which meet this criterion at liquid nitrogen temperatures at voltages two or more times the voltage required to deplete the detector. Sometimes, particularly when the humidity was high, the lowest leakage current was obtained when the detector was warmed to ~ 100°C for about 30 min before being mounted in the cryostat.

The largest detector we fabricated (5.3 cm^2 x 0.74 cm thick) is a simple cylindrical planar structure with 1 nA leakage current at 600 V (depletion voltage of ~ 30 V). A lateral scan with a slit-collimated ^{137}Cs γ-ray beam was made (Fig. 7). Comparison of the active thickness at 10, 20, 30, and 400 V indicates that nearly

Figure 7 Integrated counts in the full-energy peak versus position for a side scan of cylindrical Ge detector GLR 156 P1 using a slit collimated ^{137}Cs (E_γ = 662 keV) source. The curves are for four different voltages and the detector was almost fully depleted at ~ 30 V.

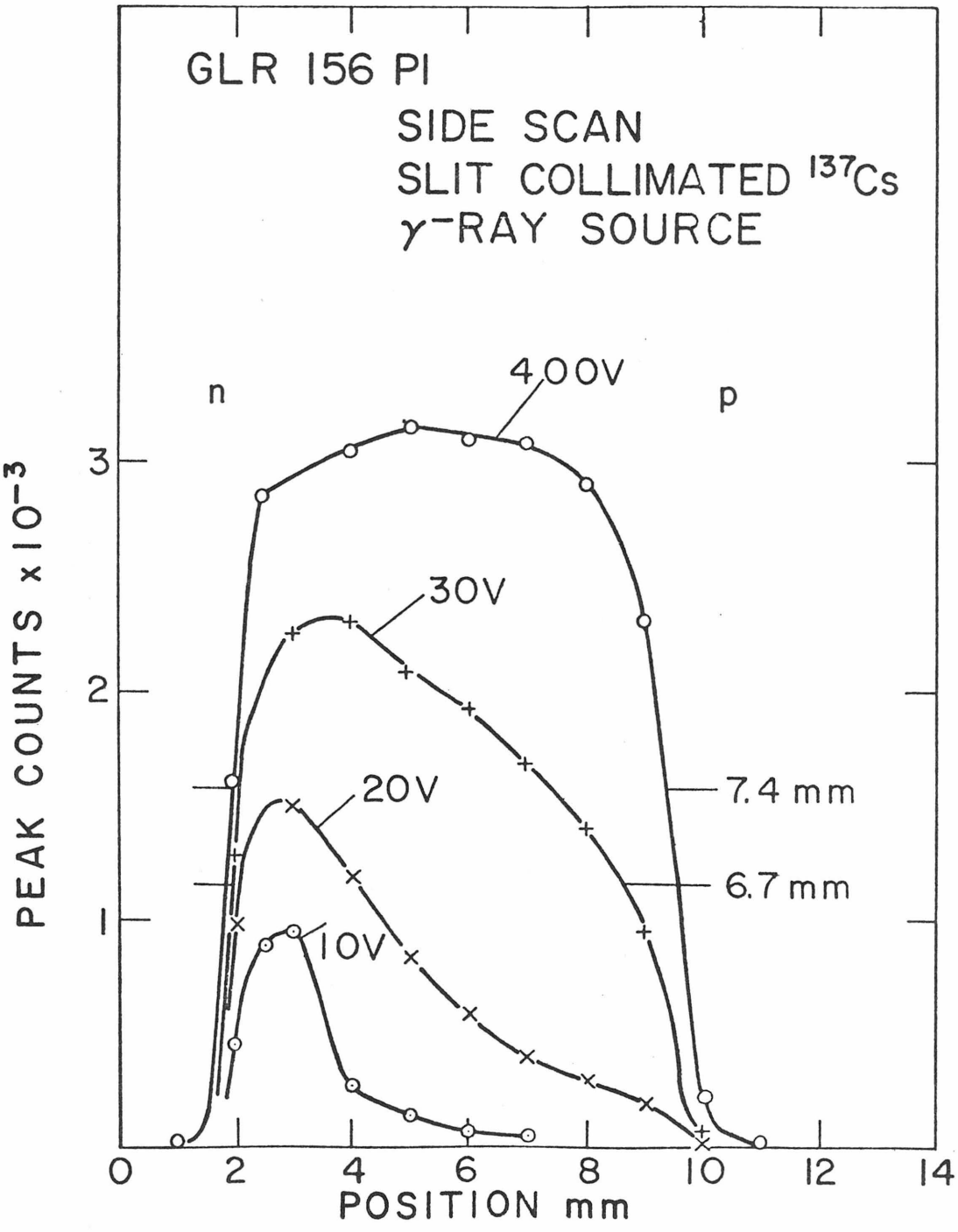
GLR 156 PI
SIDE SCAN
SLIT COLLIMATED ^{137}Cs
γ-RAY SOURCE
n
p
400V
30V
20V
10V
7.4 mm
6.7 mm
PEAK COUNTS x 10^{-3}
POSITION mm
0
2
4
6
8
10
12
14
1
2
3

Figure 7

full depletion was obtained at 30 V. Surface scans of the Al p contact with a spot-collimated ^{241}Am 59.5 keV γ-ray source (Fig. 8) showed that almost all the surface was active at applied voltages greater than the depletion voltage; some detectors tended to deplete first in the central regions.

Figures 9 and 10 show γ-ray spectra on an 8 mm thick detector of active area 2.7 cm^2. Full depletion (7.4mm) was obtained at 320 V. The leakage current was less than 1 nA at 600 V. The energy resolution for ^{57}Co at 122 keV was 0.97 keV (Fig. 9) and for ^{60}Co was ~ 2 keV (Fig. 10). The applied voltage was the same for both spectra (350 V); the difference in pulser width is due to changes in electronics. These results are comparable to those obtained with other Ge detectors operated in the same electronic system.

There was no evidence that the temperature cycle during processing degraded the material properties. Spectra from slices of germanium reprocessed three or more times did not have features associated with trapping effects such as pulse height shifts or tails below the γ-ray peaks.

Estimates of the window thickness were made by comparing the pulse height response to 5.486 MeV α-particles to the energy calibration curve obtained by using γ-rays from an ^{241}Am source. The measured peak shift of 38 keV corresponds to an aluminum window thickness of 0.25 μm of germanium. In this work no attempt was made to minimize window thickness as the objective was to evaluate gamma response.

Figure 8 Similar curves to those of Fig. 7 but using a spot collimated ^{241}Am (E_γ= 59.6 keV) source to scan across the circular Al contact face of the detector. The lower count rate at the center is due to attenuation from the contact lead and mylar strap used to hold the detector.

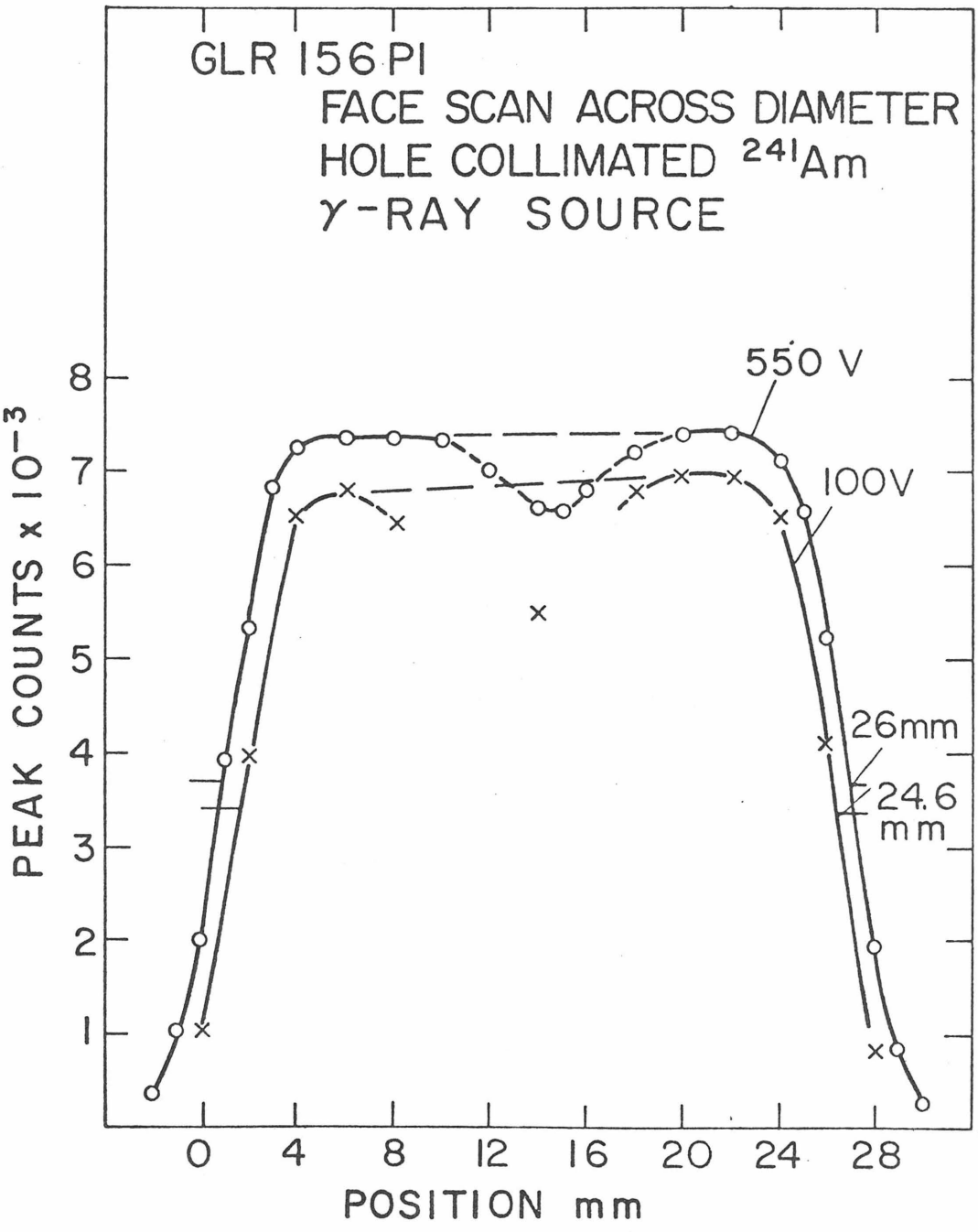
GLR 156 PI
FACE SCAN ACROSS DIAMETER
HOLE COLLIMATED ^{241}Am
γ-RAY SOURCE
550 V
100V
26mm
24.6
mm
PEAK COUNTS x 10^{-3}
1
2
3
4
5
6
7
8
0
4
8
12
16
20
24
28
POSITION mm

Figure 8

Figure 9 Spectrum of γ-rays from a combined ^{241}Am and ^{57}Co sources for Ge detector G1101 P3.

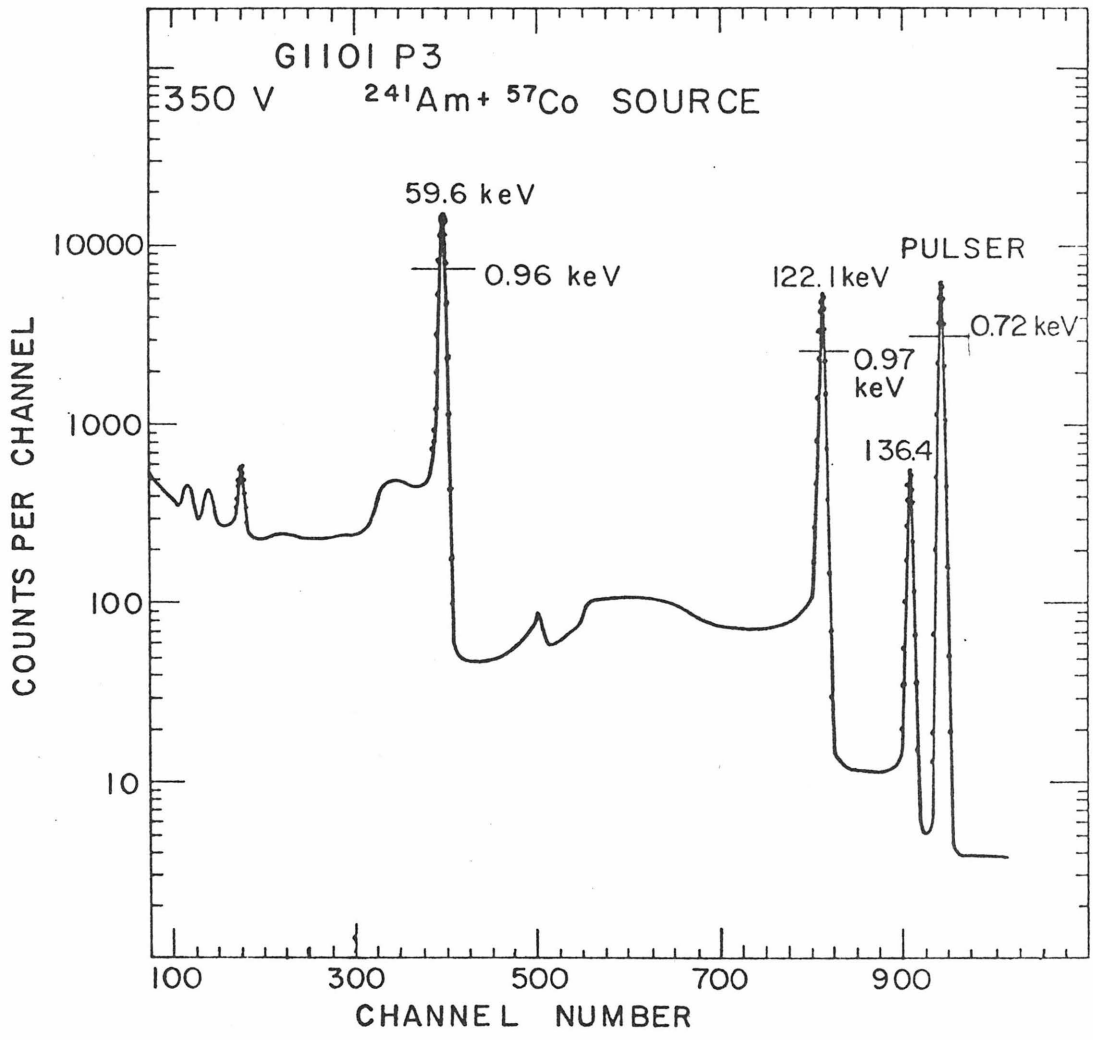
G1101 P3
350 V
241Am+ 57Co SOURCE
59.6 keV
0.96 keV
122.1keV
0.97 keV
PULSER
0.72 keV
136.4
10000
1000
100
10
COUNTS PER CHANNEL
100
300
500
700
900
CHANNEL NUMBER

Figure 9

Figure 10 Part of the γ-ray spectrum from a ^{60}Co source taken with Ge detector G1101 P3.

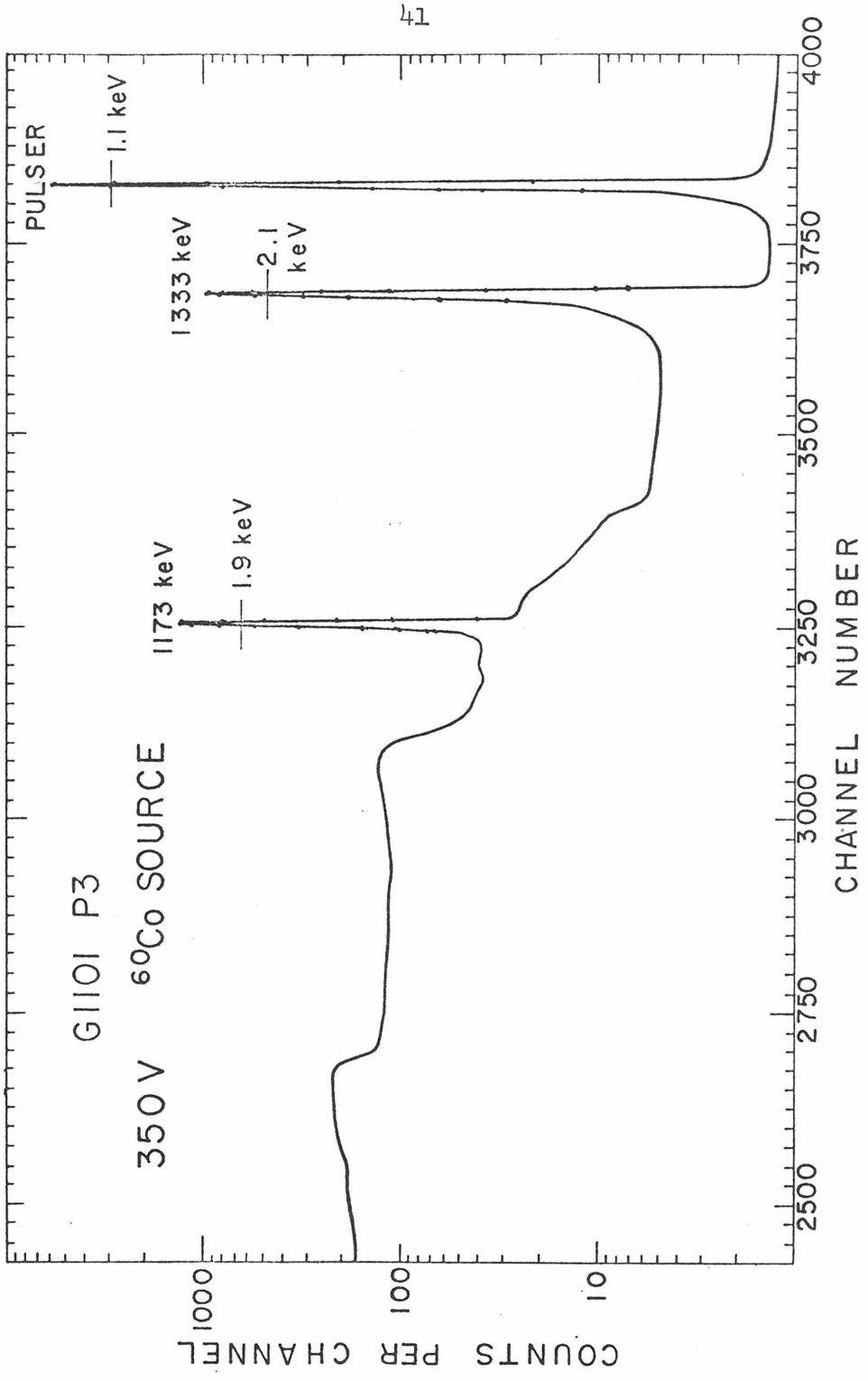
PULSER
1.1 keV
1333 keV
2.1 keV
1173 keV
1.9 keV
G1101 P3
350 V
60Co SOURCE
COUNTS PER CHANNEL
1000
100
10
2500
2750
3000
3250
3500
3750
4000
CHANNEL NUMBER

Figure 10

As shown in Fig. 11, the resolution for the 5.5 MeV α-particles was 30 keV fwhm. In other studies [32,47] window thicknesses less than 0.1 μm and better α-particle resolution ($\sim$ 13 keV) have been achieved.

3. Conclusion

The objective of this study was to determine if regrowth techniques could be used to make large area, high quality, blocking contacts capable of withstanding high electric fields. The fabrication procedure should not degrade the charge collection properties of high purity Ge. We believe that our results indicate that regrowth techniques can be used.

B. Ge Double Injection Diodes

In this part of Section IV we study the hole injecting properties of the p-type Ge layers. It has been shown in Part A of this Section that the Ge layers form high quality, large area, blocking contacts on high-purity Ge γ-ray detectors. The hole injecting properties of these layers into high-purity Ge is investigated by fabricating and evaluating Ge double injection diodes in the temperature range from 77 ^{o}K to 300 ^{o}K. A test of the hole injecting nature of the Ge layer was obtained by comparing the experimental results with the predictions of double injection theory.

Figure 11 Spectrum of α-particles from a ^{241}Am source incident on the Al contact of detector G1101 P3 operating at 600 V. Using the γ-rays from an ^{241}Am source for calibration, the pulse peak defect of 38 keV for the α-particles indicated a window thickness equivalent to 0.25 μm of Ge.

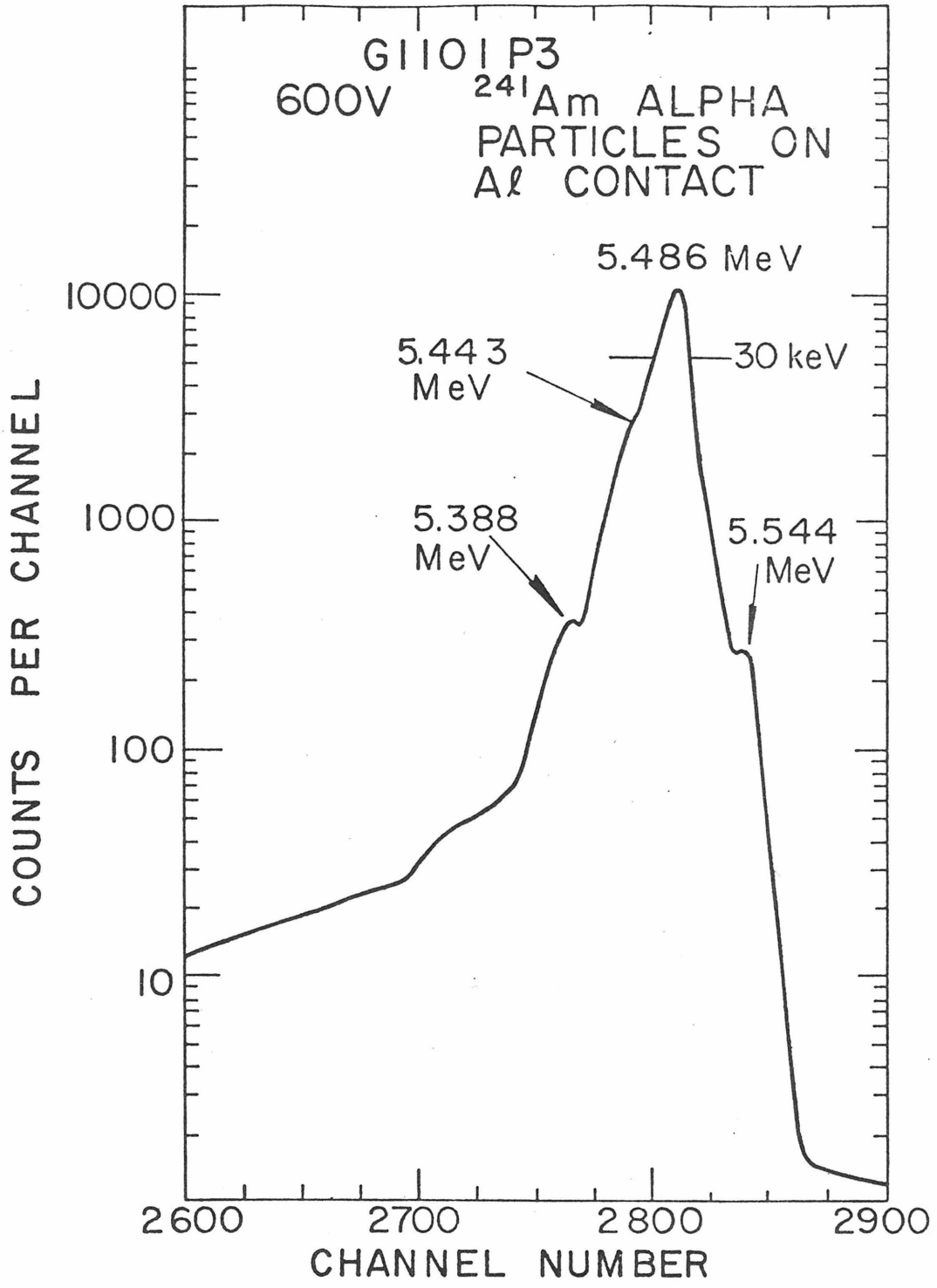
G1101P3
600V
241Am ALPHA
PARTICLES ON
Aℓ CONTACT
5.486 MeV
30 keV
5.443
MeV
5.388
MeV
5.544
MeV
10000
1000
100
10
COUNTS PER CHANNEL
2600
2700
2800
2900
CHANNEL NUMBER

Figure 11

1. Double Injection Considerations

Double injection theory for semiconductors predicts a number of current-voltage regimes.[48] Some of these are the ohmic, semiconductor and diffusion regimes. The ohmic regime is observed at low applied voltage where no appreciable injection occurs. The diffusion regime is hard to characterize quantitatively due to the difficulty in measuring some of the necessary parameters. However, for the semiconductor regime, all the necessary parameters are either available or can be easily measured. Therefore, it is convinient to use the semiconductor regime to demonstrate the hole injecting nature of the grown Ge layers.

The steady-state current-voltage characteristics of a double injection diode made from a n-type semiconductor is

$$I = 9\, A\, e\, \mu_n\, \mu_p\, N_d\, \tau\, V^2 / 8\, L^3 \qquad \text{IV - 1}$$

where I is the current, V the voltage across the lightly doped region, A the cross-sectional area, L the distance between the voltage probes across the lightly doped region, e the electron charge, μ_n the electron mobility, μ_p the hole mobility, τ the common high level injection lifetime and N_d the net donor concentration in the lightly doped region. The current, voltage, area and length can be directly measured. The net donor concentration can be calculated from the ohmic conductivity and the published values of the carrier mobilities.[49,50] The common high level injection lifetime can be measured from the small signal current transients.[48] The small

signal current transient is obtained by applying a small voltage pulse on top of a DC bias to the double injection diode. In the semiconductor regime, after a short ohmic relaxation time, the small signal current changes exponentially with time. The time constant is the common high level injection lifetime.

2. Experimental Results

Ge double injection diodes were made using techniques similar to the fabrication of Ge γ-ray detectors discussed in Part A of this Section. Double injection diodes were made from a lightly-doped Ge bar with a hole and electron injecting contacts on opposite ends. Ge crystals with net concentrations in the range of 10^{10} to $10^{12}/cm^3$ were used. The double injection diodes were operated from 77 to 300°K.

The measured current-voltage characteristics of a 0.166 cm^2 by 2.42 cm long Ge double injection diode made with n-type Ge is shown in Fig. 12. The voltage probe spacing is 2.22 cm. The current-voltage characteristics were measured at 215 °K (circles), 150 °K (triangles) and 110 °K (dots). The insert shows a typical small signal current transient obtained with the double injection diode biased into the semiconductor regime. Similar small signal current transients were used to measure τ at various temperatures. The results are tabulated in Table 1 along with the probe voltages at a current of 10 mA and the published electron and hole mobilities in high purity Ge[49,50].

TABLE I

Parameters used to calculate the current-voltage characteristics of a high purity, $N_d - N_a = 2.0 \times 10^{11} / cm^3$, Ge double injection diode biased in the semiconductor regime. The diode dimensions are 0.166 cm^2 by 2.42 cm long.

T	μ_n*	μ_p*	τ	V at 10 mA	I_c/I_m
°K	cm^2/Vs	cm^2/Vs	μs	V	
215	6,600	3,900	125	71	0.9
185	8,600	5,500	77	74	1.1
150	12,000	9,000	70	52	1.1
110	19,000	20,000	50	34	1.2

* Mobility values from Ottaviani et al [49,50]

Figure 12 Current-voltage charecteristics for a high purity, $N_d - N_a = 2.0 \times 10^{11}$ /cm^3, Ge double injection diode measured at 215 °K, 150 °K and 110 °K. The insert shows a small signal current transient at 170 °K with the diode biased at 10 mA.

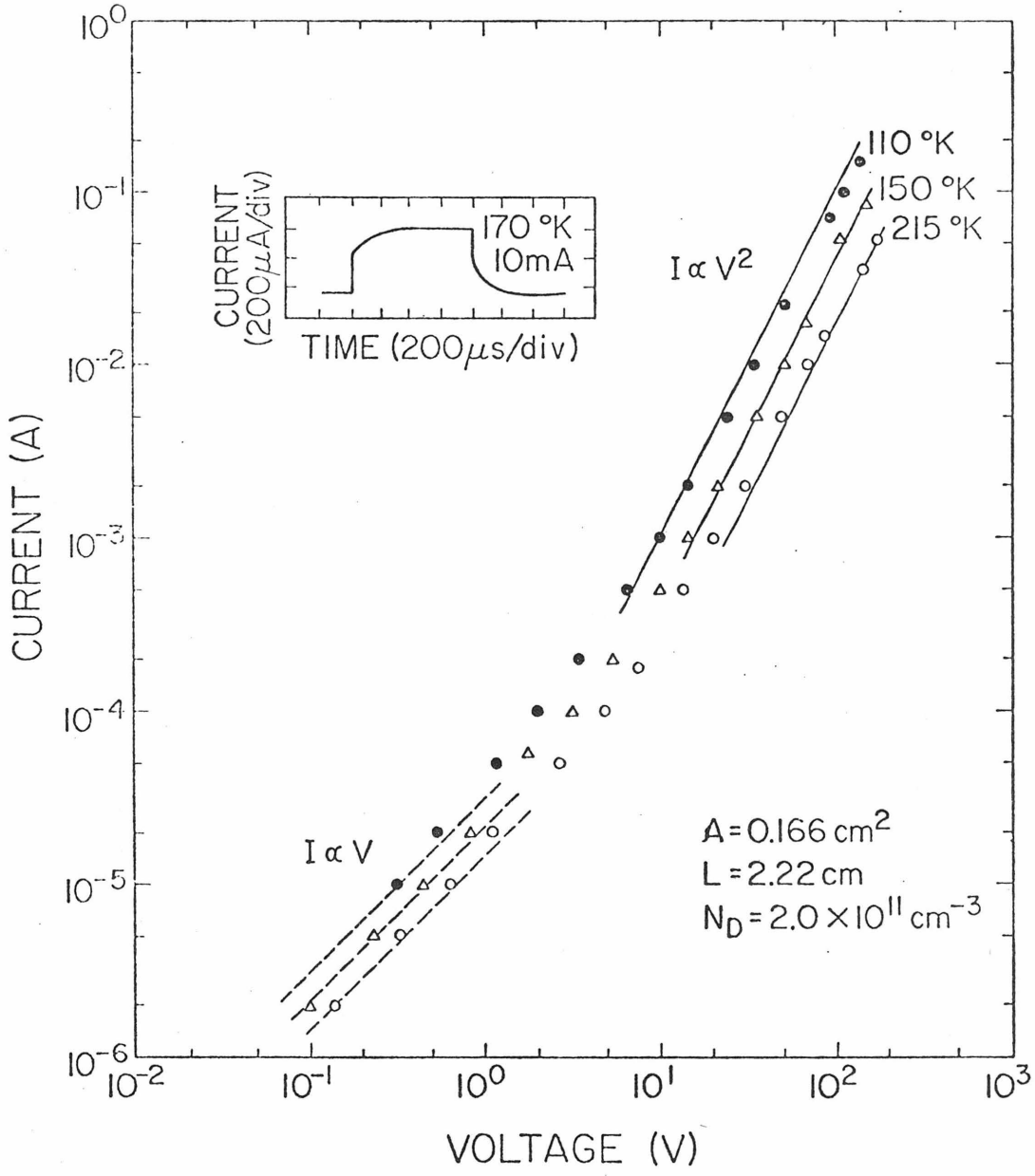
CURRENT (A)
VOLTAGE (V)
110 °K
150 °K
215 °K
I ∝ V²
I ∝ V
CURRENT (200μA/div)
TIME (200μs/div)
170 °K
10mA
A = 0.166 cm²
L = 2.22 cm
N_D = 2.0 × 10¹¹ cm⁻³

Figure 12

A net donor concentration of 2.0×10^{11} /cm^3 was calculated for this device using the measured ohmic conductivity and the electron mobility. This value is in good agreement with Hall effect measurements at 77 ^{o}K(51). The calculated current-voltage characteristics (shown as a solid lines in Fig. 12) were calculated using equation IV - 1 and values shown in Table 1. Table 1 shows the measured probe voltage at a current of 10 mA and the ratio of the calculated to measured currents at these voltages. One can see from Table 1 and Fig. 12 that the experimental data agrees well with the calculated values.

3. Conclusions

Ge/Al solid-phase p-type layers form good hole injecting contacts in the temperature range from 77 to 300 ^{o}K. Double injection theory agrees well with experimental current-voltage characteristics.

REFERENCES

1. A. J. Khambata, Introduction to Integrated Semiconductor Circuits, (John Wiley and Sons, Inc., New York, 1963).
2. C. J. Kircher, Solid-State Electron., 14, 507 (1971).
3. W. D. Buckley and S. C. Moss, Solid-State Electron., 15, 1331 (1972).
4. R. W. Bower, Solid-State Electron., 16, 146 (1973).
5. J. Gyulai, J. W. Mayer, V. Rodriquez, A. Y. C. Yu, and H. J. Gopen, J. Appl. Phys., 42, 3578 (1971).
6. T. Kawamura, D. Shinuda, and H. Muta, Appl. Phys. Lett., 11, 101 (1967).
7. R. A. Tolla and R. P. Sopher, IBM J. Res. Dev., 13, 226 (1969).
8. A. Hiraki, M-A. Nicolet, and J. W. Mayer, J. Appl. Phys., 42, 4378 (1971).
9. J. O. McCaldin and H. Sankur, Appl. Phys. Lett., 20, 171 (1972).
10. J. M. Caywood, Met. Trans., 4, 735 (1973).
11. J. M. Caywood, A. M. Fern, J. O. McCaldin, and G. Ottaviani, Appl. Phys. Lett., 20, 326 (1972).
12. J. O. McCaldin and H. Sankur, Appl. Phys. Lett., 19, 524 (1971).
13. H. Sankur, J. O. McCaldin, and J. Devaney, Appl. Phys. Lett., 22, 64 (1973).
14. A. Hiraki, E. Lugujjo, M-A. Nicolet, and J. W. Mayer, Phys. Status Solidi, A7, 401 (1971).

15. A. Hiraki, E. Lugujjo, and J. W. Mayer, J. Appl. Phys., 43, 3643 (1972).

16. R. W. Bower and J. W. Mayer, Appl. Phys. Lett., 20, 359 (1972).

17. R. W. Bower, Appl. Phys. Lett., 23, 99 (1973).

18. C. J. Kircher, J. W. Mayer, K. N. Tu, and J. F. Ziegler, Appl. Phys. Lett., 22, 81 (1973).

19. M. Tannenbaum, Semiconductors, N. B. Hannay, Ed. (Reinhold, New York, 1959), p. 87.

20. J. H. Broghy, R. M. Rose, and J. Wulff, Structures and Properties of Materials, J. Wulff, Ed. (Wiley, New York, 1964), Vol. 12, p. 112.

21. K.H. Henisch, Crystal Growth in Gels, (Pennsylvania State Univ. Press, University Park, 1970).

22. R. A. Laudisse, J. R. Carruthers, and K. A. Jackson, Annu. Rev. Mater. Sci., I, 253 (1971).

23. V. Marrello, J. M. Caywood, J. W. Mayer, M-A. Nicolet, Phys. Status Solidi, 13, 531 (1972).

24. G. Ottaviani, D. Sigurd, V. Marrello, J. O. McCaldin, Science, 180, 948 (1973).

25. D. Sigurd, G. Ottaviani, V. Marrello, J. W. Mayer, and J. O. McCaldin, J. Non. Cryst. Solids, 12, 135 (1973).

26. G. Ottaviani, D. Sigurd, V. Marrello, J. W. Mayer, and J. O. McCaldin, J. Appl. Phys., 45, 1730 (1974).

27. M. Hansen, Constitution of Binary Alloys, (McGraw-Hill Publishing

Co., 1958), p. 96.

28. H. S. Chen and D. Turnbull, J. Appl. Phys., 40, 4214 (1969).

29. E. W. Williams and H. B. Bebb, Semiconductors and Semimetals, Willardson and Beer, Ed. (Academic, New York, 1972) Vol. 8, Chap. 5.

30. L. R. Dawson, Progress in Solids State Chem., Reiss and McCaldin, Ed. (Pergamon, New York, 1972) Vol. 7, pg. 117.

31. A. S. Grove, Physics and Technology of Semiconductor Devices, (Wiley, New York, 1973) Chp. 1.

32. G. Ottaviani, V. Marrello, J. W. Mayer, M-A. Nicolet, and J. M. Caywood, Appl. Phys. Lett., 20, 323 (1972).

33. J. M. Caywood, A. M. Fern, J. O. McCaldin, and G. Ottaviani, Appl. Phys. Lett., 20, 326 (1972).

34. A. M. Fern and J. O. McCaldin, Proc. IEEE, 60, 1018 (1972).

35. V. Marrello, T. A. McMath, J. W. Mayer, and I. C. Fowler, Nuc. Inst. Meth., 108, 93 (1973).

36. N. G. E. Johansson, J. W. Mayer, and O. J. Marsh, Solid State Electronics, 13, 317 (1970).

37. O. A. Golikava, B. Ya. Moizhes, and A. G. Orlov, Soviet Phys. Solid State, 4, 2550 (1963).

38. F. A. Trombore and A. A. Tartaglia, J. Appl. Phys., 29, 1511 (1958).

39. R. P. Elliott, Constitution of Binary Alloys, 1st Suppl., (mcGraw-Hill Publ. Co., 1965) p 38.

40. W. Meer and P. Pommerrenig, Z. angew. Phys., 23, 369 (1967).

41. S. T. Picraux, J. A. Davies, L. Eriksson, N. G. E. Johansson, and

J. W. Mayer, Phys. Rev., 180, 873 (1969).

42. T. M. Donovan, E. J. Ashley and W. E. Spicer, Phys. Lett., 32A, 85 (1970).

43. T. M. Donovan, Ph.D. Thesis, Stanford University, 1970.

44. M-A. Nicolet, J. W. Mayer, and I. V. Mitchell, Science, 177, 841 (1972).

45. C. Canali, J. W. Mayer, G. Ottaviani, D. Sigurd and W. van der Weg, Appl Phys. Lett., 25, 3 (1974).

46. G. T. Ewan and A. J. Tavendale, Can. J. Phys., 42, 2268 (1964).

47. A. Lidow, Undergraduate Research Program, CIT (1973).

48. R. Baron and J. W. Mayer, Semiconductors and Semimetals, Willardson and Beerd, Ed. (Academic, New York, 1970) Vol. 6, Chap. 4.

49. G. Ottaviani, C. Canali, F. Nava, and J. W. Mayer, J. Appl. Phys., 44, 2917 (1973).

50. L. H. De Laet, W. K. Schoemaekers, H. J. Guislain, and M. Meens, Second Symposium on Sem. Detect. for Nucl. Rad., Munich 6-9, Sept. 1971.

51. R. N. Hall,(GE Research and Development Center, Schenectady) private communication.

PART II

CONDENSATION OF INJECTED ELECTRONS AND HOLES IN GERMANIUM

I: INTRODUCTION

Photon or electron beams impinging on Ge surfaces have been used to excite electrons and holes in Ge[1]. A fraction of these electrons and holes bind into excitons. This fraction increases as the temperature is lowered. One way these excitons can recombine is to emit a phonon and a photon. LA- and TO- phonon assisted exciton recombination radiation at 714 meV and at 706 meV respectively has been observed over a wide range of temperatures.

At high excitation levels a new, broad, lower energy peak is observed in the recombination radiation spectrum of Ge at liquid He temperatures[2]. These new peaks in the spectrum have been identified as being due to LA- and TO- phonon assisted recombination radiation from a higher density phase (condensate) of electrons and holes.[2-6] The LA- and TO- phonon assisted condensate recombination lines occur at 709 meV and at 700 meV respectively.

Other techniques which have been used to study the condensation of electrons and holes include Rayleigh scattering of optical beams,[3,7] noise spikes in the reverse current of p-n junction[8], cyclotron resonance[9] and monitoring the plasma radiation[10]. Rayleigh light scattering experiments indicate that the condensation of electrons and holes occurs in the form of droplets when produced by photon beam excitation. They also suggest that the droplets are of micron sizes. A density of $2 \times 10^{17}/cm^3$ electron-hole pairs in the condensate has

been measured independantly from line fits to the recombination radiation spectrum[3] and from the plasma frequency measurements.[10] Experiments which measure noise spikes in the reverse current of a p-n junction suggests that a droplet contains 10^6 to 10^8 electron-hole pairs.[8] The recombination radiation lifetime was measured to be 40 μs in the purest Ge crystals and as low as 8 μs in other crystals.[3,5,9]

The binding energy of the condensate with respect to the excitons has been measured in two ways. One method was to measure the threshold photon beam power for condensate formation as a function of temperature[8,9] (coexistence curve method). The other method was to measure the separation in energy between the exciton and condensate recombination radiation peaks[3] (spectroscopic method). The reported values of the binding energy are 1.5 meV[8,9] and 2.6 meV[3] respectively. A critical temperature of 6.5 °K and a critical density of $8 \times 10^{16}/cm^3$ for the condensate have been measured.[11] The properties of the condensed phase in Ge are summerized in Table 1.

The condensation of electrons and holes in Ge has been interpreted in terms of a first order transition between an exciton gas and a metallic electron-hole Fermi liquid.[12-17] Theoretical models have been proposed and calculations made to explain and predict the physical properties of the condensate. The calculations indicate that the metallic electron-hole condensate is more strongly bound than either excitons or excitonic molecules at low temperature. They predict a critical temperature of between 5.6 to 8 °K and a critical density

TABLE I

PROPERTIES OF THE CONDENSATE IN Ge

Pair Density	
a) Spectroscopic	2 x 10^{17}/ cm^3
b) Plasma frequency	2 x 10^{17}/ cm^3
Binding Energy Per Pair	
a) Spectroscopic	2.6 meV
b) Coexistance Curve	1.5 meV
Critical Temperature	~ 8°K
Lifetime	
a) Condensate	40 μs
b) Exciton	~ 1 μs
Radiative Efficiency	
a) Condensate	~ 50 %
b) Exciton	~ 1 %

of between 7×10^{16} to $9.3 \times 10^{16}/cm^3$ for the condensate. The binding energy of the condensate with respect to the excitons is calculated to be between 1.4 meV and 2.0 meV. A density of $2 \times 10^{17}/cm^3$ is predicted for the condensate in Ge at 4.2 ^{o}K.

Part II of this thesis deals with the condensation of electrons and holes in Ge produced by electrical injection of electrons and holes into bulk Ge crystals.[18,19] The structure used was double injection diode made from high purity Ge crystals.

In this work the properties of the condensate produced by the electrical injection of carriers are investigated. Included are studies of direct and pulsed current excitation, recombination radiation spectra at various temperatures, current and temperature dependance of the condensate's recombination radiation intensity, decay kinetics of the recombination radiation from excitons and condensate, and spatial distribution of the recombination radiation intensity in the Ge double injection diodes. The current-voltage characteristics of the double injection diodes were measured at various temperatures.

II. EXPERIMENTAL

A. Device Fabrication

Double injection diodes for the electron-hole condensate study were made from n-type and p-type high purity Ge, $|N_a - N_d| \sim 10^{10}$ to $10^{11}/cm^3$. In the first experiments double injection Ge diodes were made in the form of a bar with cross-sectional area of 1 to $4mm^2$ and 1 to 4 mm long. Electron injecting, Li-diffused n-contacts and hole injecting, solid-phase Al p-contacts were made on opposing faces (see Part 1, Section IV of this thesis). The Li contact was indium soldered to a Cu plate and a Cu wire was indium soldered to the Al contact.

Later, to improve the heat dissipation, the double injection diodes were made on quarter slices of high purity Ge. The Ge slices are 100 to 200 mm^2 in area and 0.6 to 5 mm thick. The Ge slices were lapped with 5 μm size grit and cleaned sequentially in trichloroethylene, acetone, and methanol ultrasonic baths and then dried. One face of the Ge slices was masked with plastic tape and then chemically etched in $3HNO_3$:1HF for 2 min. The etch was quenched with methanol, plastic tape removed and the slices were placed in HF. They were rinsed with methanol and dried prior to loading them into an evaporator. An Al film, 0.5 μm thick, was evaporated on the chemically etched side of the slices. The opposite side of the slice was painted with a Li in mineral oil suspension and the slice placed in

a quartz tube furnace having a N_2 atmosphere. They were heated at 300 °C for 20 min and than slowly cooled to room temperature (~ 1.5 °C/min). This procedure can yield a Li-diffused n contact on one side and a solid-phase Al p contact on the other side of the Ge slice.[20]

A black wax mask was used to protect the entire Li-diffused side of the Ge slices and 2 to 10 mm^2 Al contacts on the other side. Some Al contacts were located at the edge of the Ge slice while others were away from the edge. The Al mesas were isolated using a $3HNO_3$:1HF etch. The Li-diffused side was lightly lapped and contacted with In; Cu wires were indium soldered to the Al contacts. A schematic sketch of a typical double injection diode of the mesa type is shown in Fig. 1.

The Ge double injection diodes were attached mechanically to a Cu block, rinsed with methanol and dried prior to doing an experiment.

B. Device Temperature Control

A Janis variable temperature dewar equipped with quartz optical windows was used for experiments performed at temperature between 2 and 300 °K. For some experiments below 4.2 °K, a pyrex glass dewar was used. For 1.5 to 4.2 °K operation, a vacuum regulated liquid He temperature bath was used. A 500 l/min mechanical pump backed the vacuum regulator.[21] Above 4.2 °K, the Janis dewar with heated He gas was used. The temperature was controlled using a C or Pt

Figure 1 Typical Ge double injection diode of the mesa type.

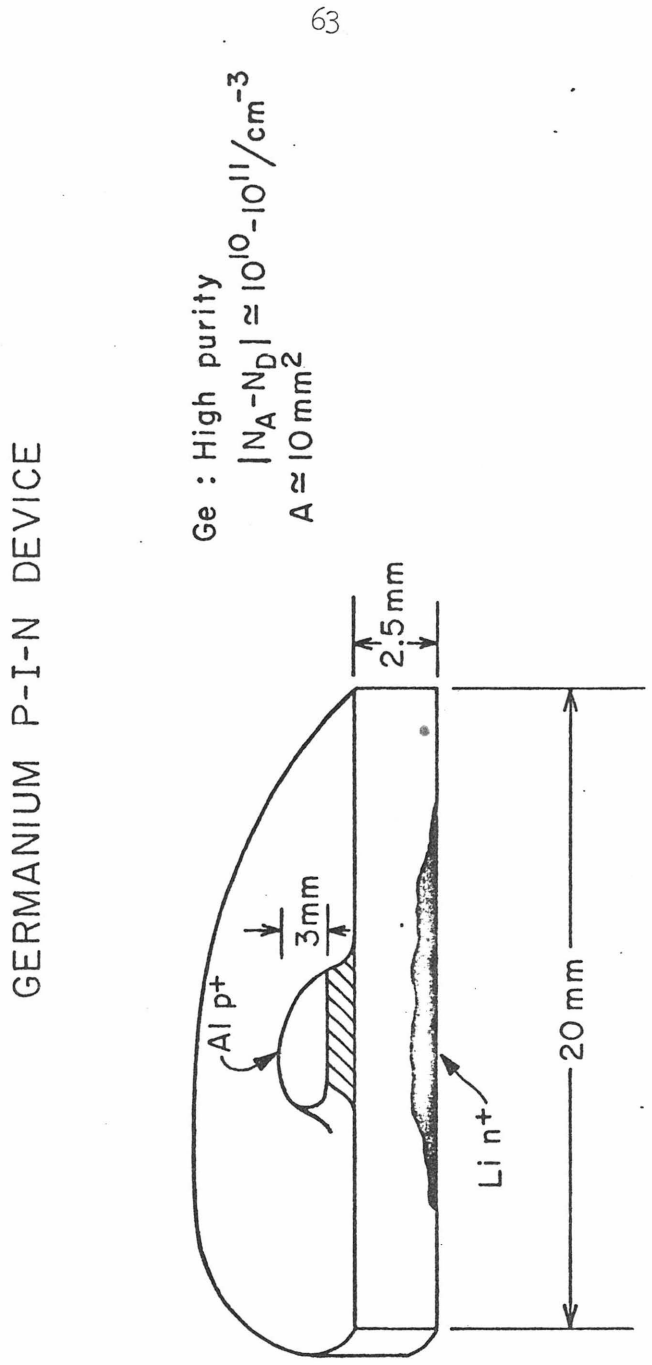
GERMANIUM P-I-N DEVICE
Ge : High purity
$|N_A-N_D| \simeq 10^{10}-10^{11}/cm^{-3}$
$A \simeq 10\,mm^2$
2.5 mm
3mm
Al p+
Li n+
20 mm

Figure 1

resistor mounted in the Cu sample block and an Artronix model 5301 temperature controller. The double injection diode temperature was measured using a calibrated Ge or Pt resistor attached to the Ge structure close to the double injection diode.

C. Measurement of the Double Injection Diode's Electrical and Optical Characteristics

The electrical and optical properties of the double injection diodes were measured using direct currents at low power levels and by using pulsed currents at higher power levels. For direct current measurements a current source was used and the voltage measured by a digital voltmeter. For pulsed currents measurements a HP 214A voltage pulser was used. The current was measured using either a HP 456A current probe or by measuring the voltage across a known resistance in series with the double injection diode. The double injection diode voltage was measured with an oscilloscope. Current pulse widths of 2 μs to 10 ms and duty cycles up to 50% were used.

The surface between the n and p contact of the double injection diode was imaged onto the entrance slit of a Spex 1400-II spectrometer. The recombination radiation from the double injection diodes was detected by an InAs or InSb photovoltaic infrared detector. For direct current measurements, the recombination radiation was detected with an InSb detector operated at 77°K along with a mechanical light chopper. For pulsed current measurements, the recombination radiation

was detected with an InAs detector operated at 195°K. The detector and preamplifier had a 0-63% response time of 1.7 μsec. The signal from the detector was processed either by a lock-in amplifier or by a box-car integrator and recorded by a strip-chart recorder. Figure 2 shows a schematic diagram of the experimental apparatus.

The spatial distribution of the recombination radiation intensity in the Ge double injection diode was measured by imaging the surface between the n and p contact onto the InAs infrared detector having a sensitive area of 0.3 mm x 1 mm. The surface area was magnified by three. The detector was mechanically scanned though the image of the surface of the double injection diode and the detector signal was processed by a lock-in amplifier and recorded by a strip-chart recorder.

Figure 2 A schematic diagram of the experimental apparatus used in electron-hole condensate experiments.

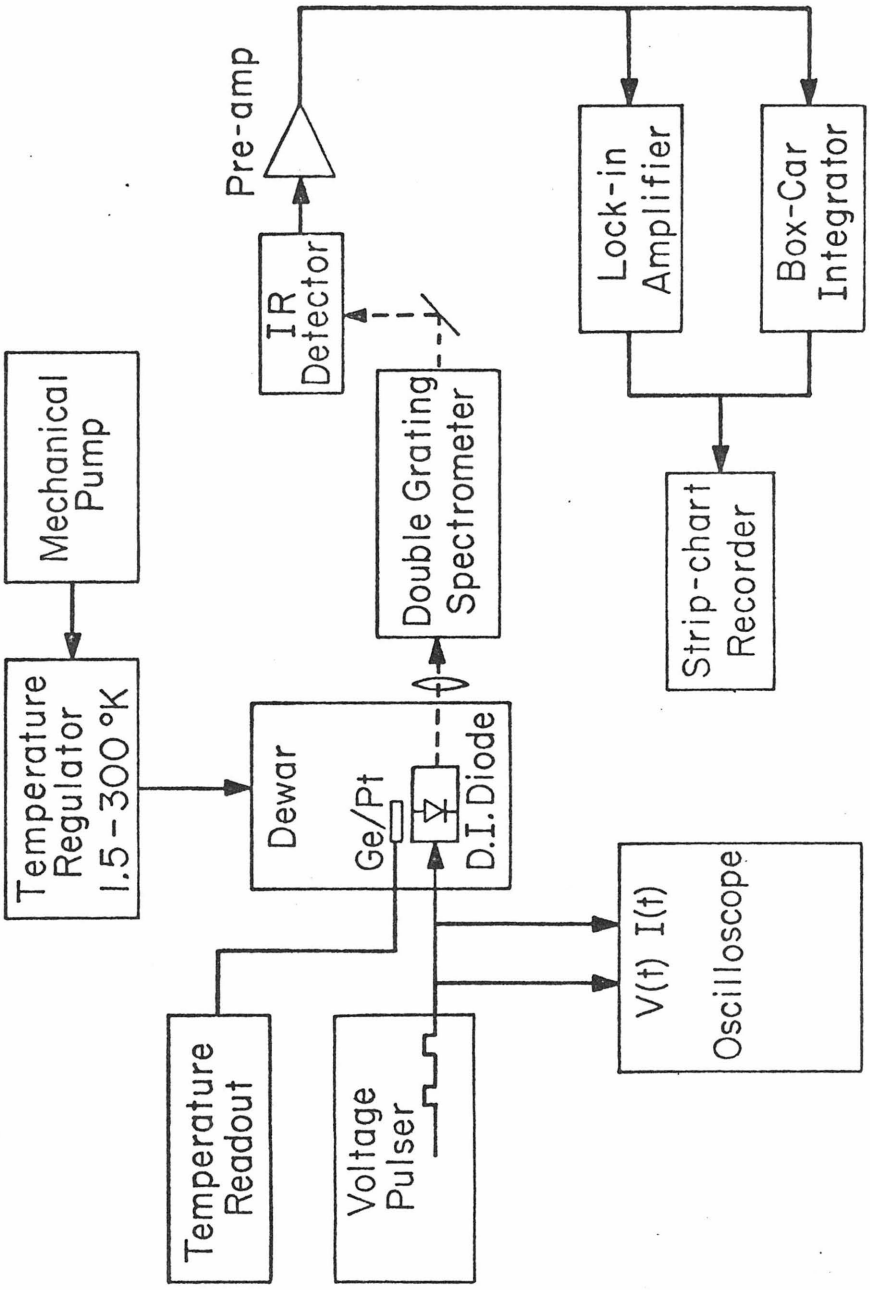
Pre-amp
IR Detector
Lock-in Amplifier
Box-Car Integrator
Mechanical Pump
Double Grating Spectrometer
Strip-chart Recorder
Temperature Regulator 1.5-300 °K
Dewar
Ge/Pt
D.I. Diode
V(t) I(t)
Oscilloscope
Temperature Readout
Voltage Pulser

Figure 2

III. RESULTS AND DISCUSSIONS

A. Electrical Characteristics of Ge Double Injection Diodes

The measured steady-state forward current-voltage characteristics of a typical Ge double injection diode used in the electron-hole condensate study is shown in Fig. 3. This particular mesa type device, Ge 201, was 2.4 mm long and located near the edge of Ge slice. Other Ge diodes of various geometries with lengths of 0.6, 1.2, and 4.7 mm showed the same general characteristics. The figure shows the current-voltage characteristics at 90°K (dot), 14°K (circle) and 4.2°K (square). The current-voltage characteristic remained nearly unchanged from 4.2°K to 1.5°K.

At 90°K the forward current increases rapidly with a small increase in applied voltage. This behavior is predicted from standard double injection theory for double injection diodes with "short" intrinsic regions (diffusion regime of double injection).[22] A double injection diode is expected to operate in a diffusion regime if the length of the device is of the order of the ambipolar diffusion length ($L_a = \sqrt{2 D_n D_p \tau/(D_n + D_p)} \sim 1$ mm at 90°K) where τ is the common high injection lifetime and D_n and D_p are the diffusion coefficients for electrons and holes respectively. The voltage dropped across the intrinsic region is usually small in these devices compared to the n and p junction voltage drops.[22] This renders the quantitative description of the current-voltage characteristics of a double

Figure 3 Forward biased, current-voltage characteristics of a 6 mm^2 by 2.4 mm long mesa type double injection diode made on a ~ 200 mm^2 area Ge slice. They were measured at 90°K (dots), 14°K (circles), and 4.2°K (squares). These rapidly rising currents versus voltage characteristics were typical of other diodes with various geometries.

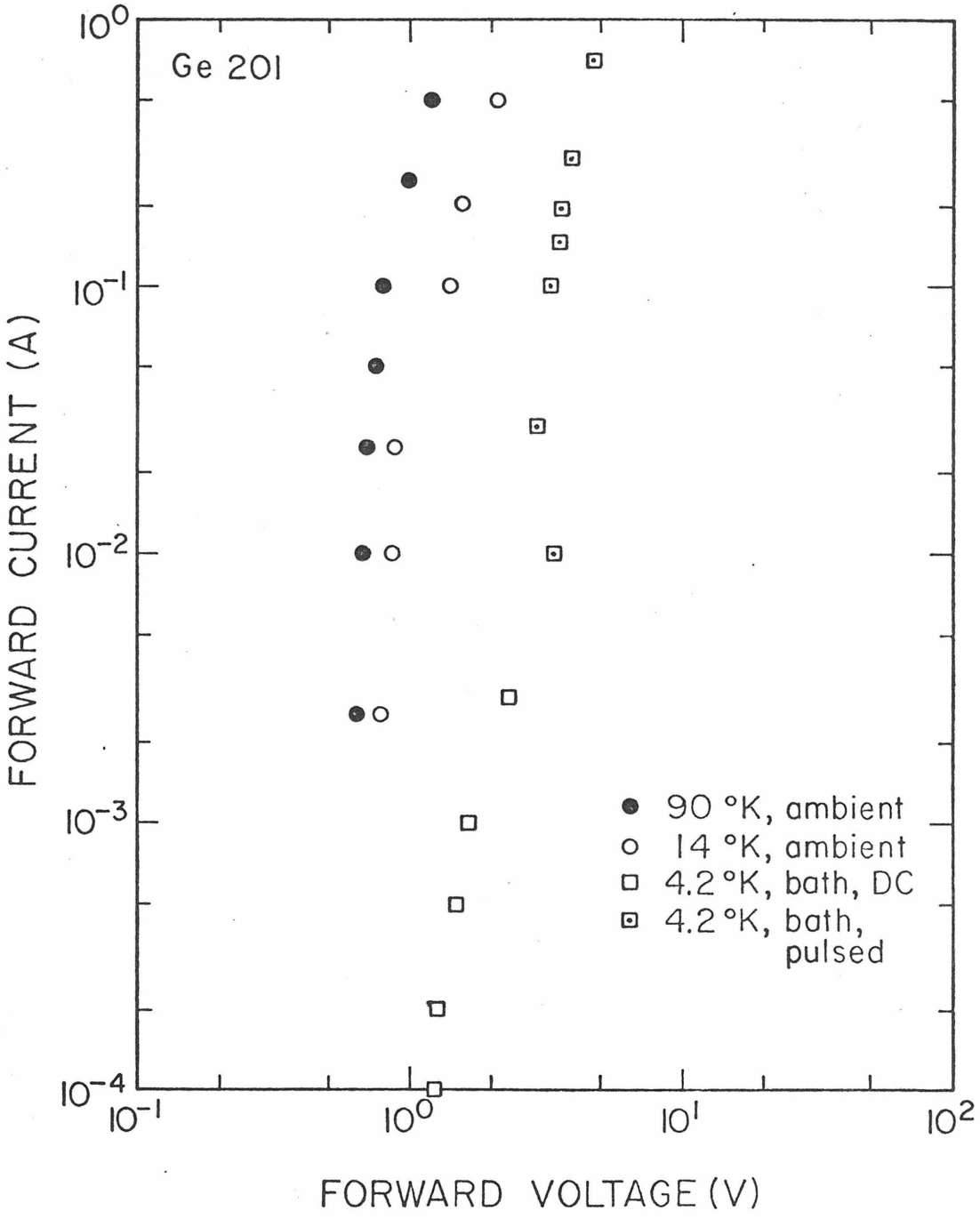
Ge 201
FORWARD CURRENT (A)
FORWARD VOLTAGE (V)
10^0
10^{-1}
10^{-2}
10^{-3}
10^{-4}
10^{-1}
10^0
10^1
10^2
90 °K, ambient
14 °K, ambient
4.2 °K, bath, DC
4.2 °K, bath, pulsed

Figure 3

injection diode difficult but qualitative agreement can be easily achieved.[23] In longer double injection diodes the voltage drop across the junctions can be made small compared with the total device voltage. In that case, quantitive agreement with standard double injection theory was achived (see Part 1, Section IV of thesis).

Standard double injection theory treats only free carrier recombination mechanisms and transport in semiconductors. However, at low temperatures, excitons, bound excitons and condensate are present in Ge double injection diodes. One might expect that they would have a significant effect on the carrier transport and could influence the current-voltage characteristics of the double injection diodes at low temperatures. At present, no double injection theory exists which takes into account free carriers, excitons and condensate. A major obstacle in formulating such a theory is that various rate kinetics between free carrier, excitons, and condensate are not fully understood.

The circles and squares in Fig. 3 are the measured current-voltage characteristics at 14°K and at 4.2°K respectively. The forward current increases rapidly with small increases in applied voltage similar to what is measured for 90°K.

B. Recombination Radiation from Ge Double Injection Diodes

The recombination radiation spectra at 20°K (dashed line) for a device current of 800 mA and at 4.2°K (solid line) for a device

current of 300 mA are shown in Fig. 4. The well established LA-phonon and TO-phonon assisted exciton recombination radiation line at 714 meV and 706 meV respectively dominate the spectrum at 20°K. At a temperature of 4.2°K, LA-phonon assisted line at 709 meV and TO-phonon assisted line at 700 meV, characteristic of the more strongly bound condensed electron-hole phase, dominate the spectrum.[3] The LA-phonon assisted exciton recombination radiation line has a linewidth at half maximum of 3.7 meV at 20°K. The LA-phonon assisted condensate recombination radiation line has a linewidth at half maximum of 3.0 meV which is essentially the same as widths reported elsewhere.[3,6] This value of the width has been used to estimate a carrier density of $2 \times 10^{17}/cm^3$ for the condensate in Ge. Similar results have been obtained with Ge double injection diodes made with various other geometries.

The condensate in the double injection diodes exists under direct and pulsed current excitation. Figure 5 shows a LA-phonon and TO-phonon assisted condensate recombination radiation spectra at 4.2°K for a pulsed and direct current of 100 mA. Both direct and pulsed current excitation of the Ge double injection diode yields similar recombination radiation spectra. Pulsed current excitation is to be preferred when device heating is of primary concern.

In summary, the condensate occurs in Ge double injection diodes at 4.2°K under direct and pulsed currents. No evidence is seen for the LA-phonon assisted exciton recombination radiation line at

Figure 4 LA- and TO-phonon assisted recombination radiation spectra of a Ge double injection diode at 20°K (dashed line) for a device current of 800 mA (11 ms pulse, 22% duty cycle) and at 4.2°K (solid line) for a device current of 300 mA (1 ms pulse, 9% duty cycle). The vertical scales are not the same for the spectra.

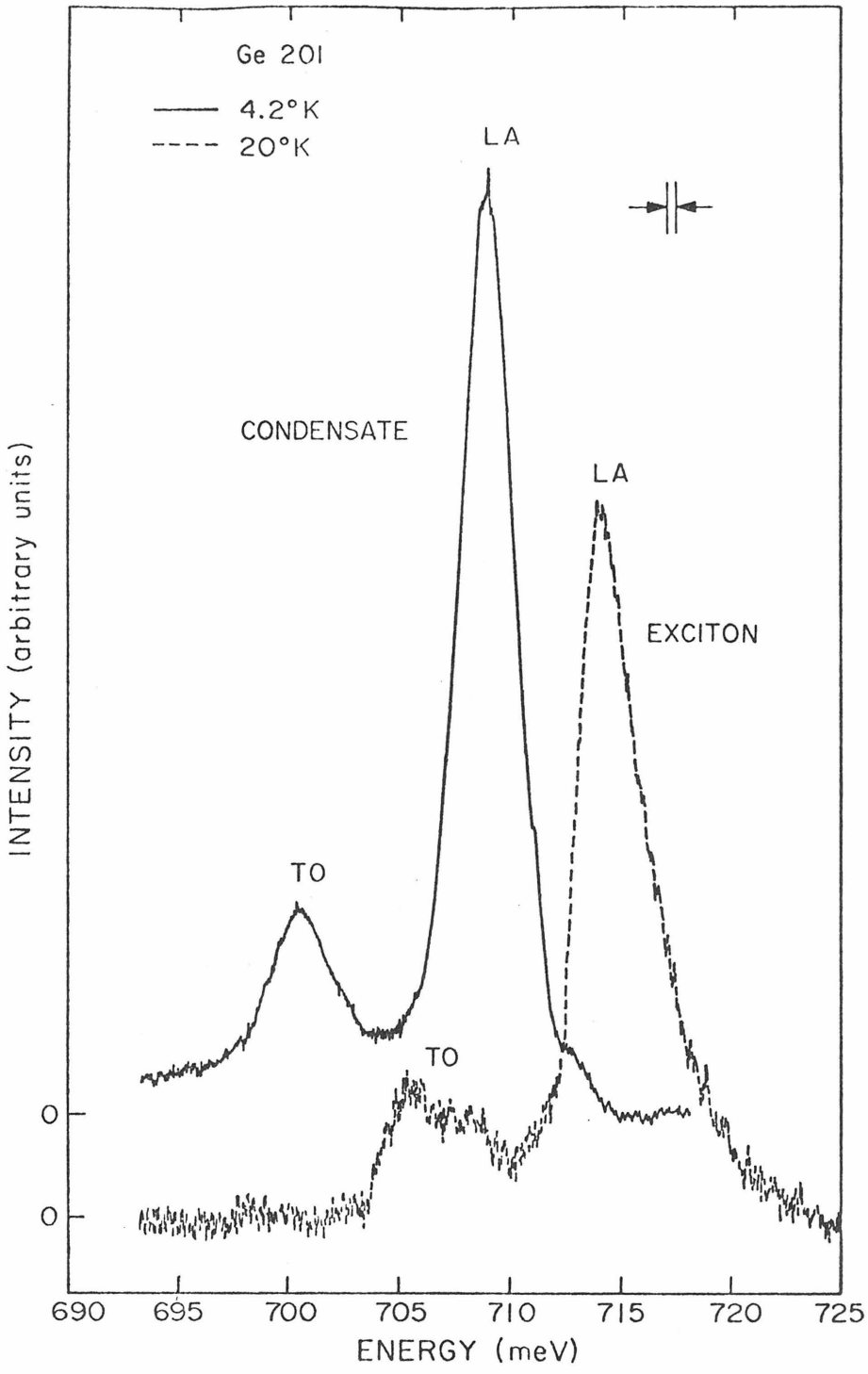
Ge 201
4.2°K
20°K
LA
CONDENSATE
LA
EXCITON
TO
TO
INTENSITY (arbitrary units)
0
0
690
695
700
705
710
715
720
725
ENERGY (meV)

Figure 4

Figure 5 LA- and TO-phonon assisted condensate recombination radiation spectra at 4.2°K for a Ge double injection diode with pulsed currents of 100 mA (4 ms pulse, 6.8% duty cycle, dashed line) and with direct current of 100 mA (solid line). The vertical scales are not the same for the spectra.

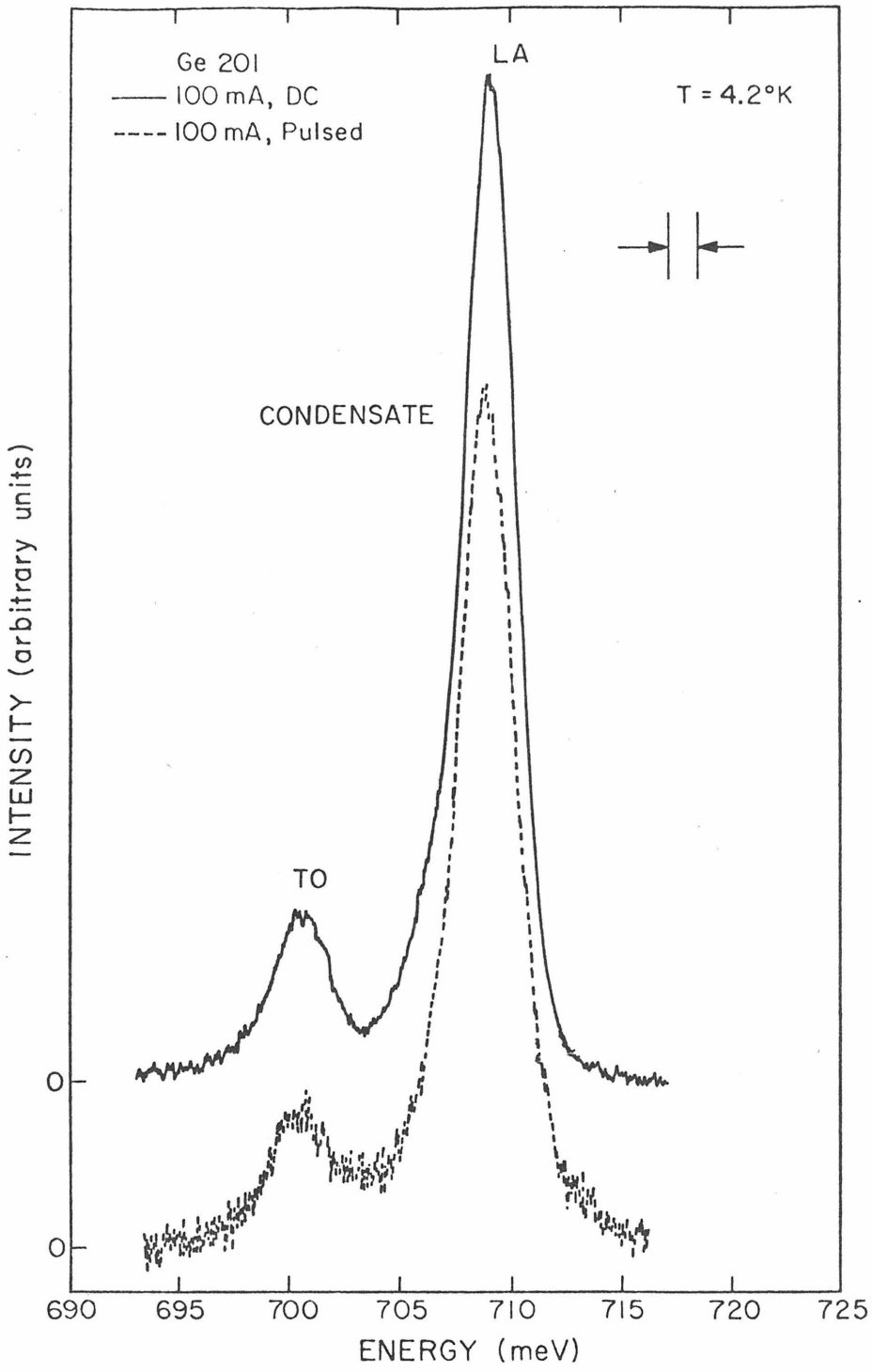
Ge 201
100 mA, DC
100 mA, Pulsed
T = 4.2°K
LA
CONDENSATE
TO
INTENSITY (arbitrary units)
0
0
690
695
700
705
710
715
720
725
ENERGY (meV)

Figure 5

714 meV for temperatures below 5°K. This is contrary to what is reported for experiments using optical beam excitation where the LA-phonon assisted exciton recombination radiation line at 714 meV has been observed for temperatures below 4.2°K. In optical excitation experiments, the presence of the exciton line could be due to surface heating or to an inhomogeneous carrier distribution.

C. Influence of Device Current and Temperature on the Recombination Radiation Spectra

The recombination radiation spectra from Ge double injection diodes were measured using direct and pulsed currents. Excitation currents in the range of 20 μA to 1.5 A were investigated. The lower current limit was imposed by the spectrometer-detector sensitivity while the higher current limit was determined by device heating considerations. These limits varied with different device structures.

1. Current Dependence

The LA- and TO-phonon assisted condensate recombination spectra at 4.2°K for a direct current of 0.2 mA (dotted), 1.0 mA (dashed) and 100 mA (solid) are shown in Fig. 6. The recombination radiation spectra show the LA- and TO-phonon assisted lines at 709 meV and 700 meV respectively. The energy position and linewidth at half maximum of the condensate lines are independent of current.

To minimize heating, higher current excitation was studied

Figure 6 LA-and TO-phonon assisted condensate recombination radiation spectra of a Ge double injection diode at 4.2°K with direct currents of 0.2 mA (dotted line), 1.0 mA (dashed line), and 100 mA (solid line). The vertical scales are not the same for the spectra.

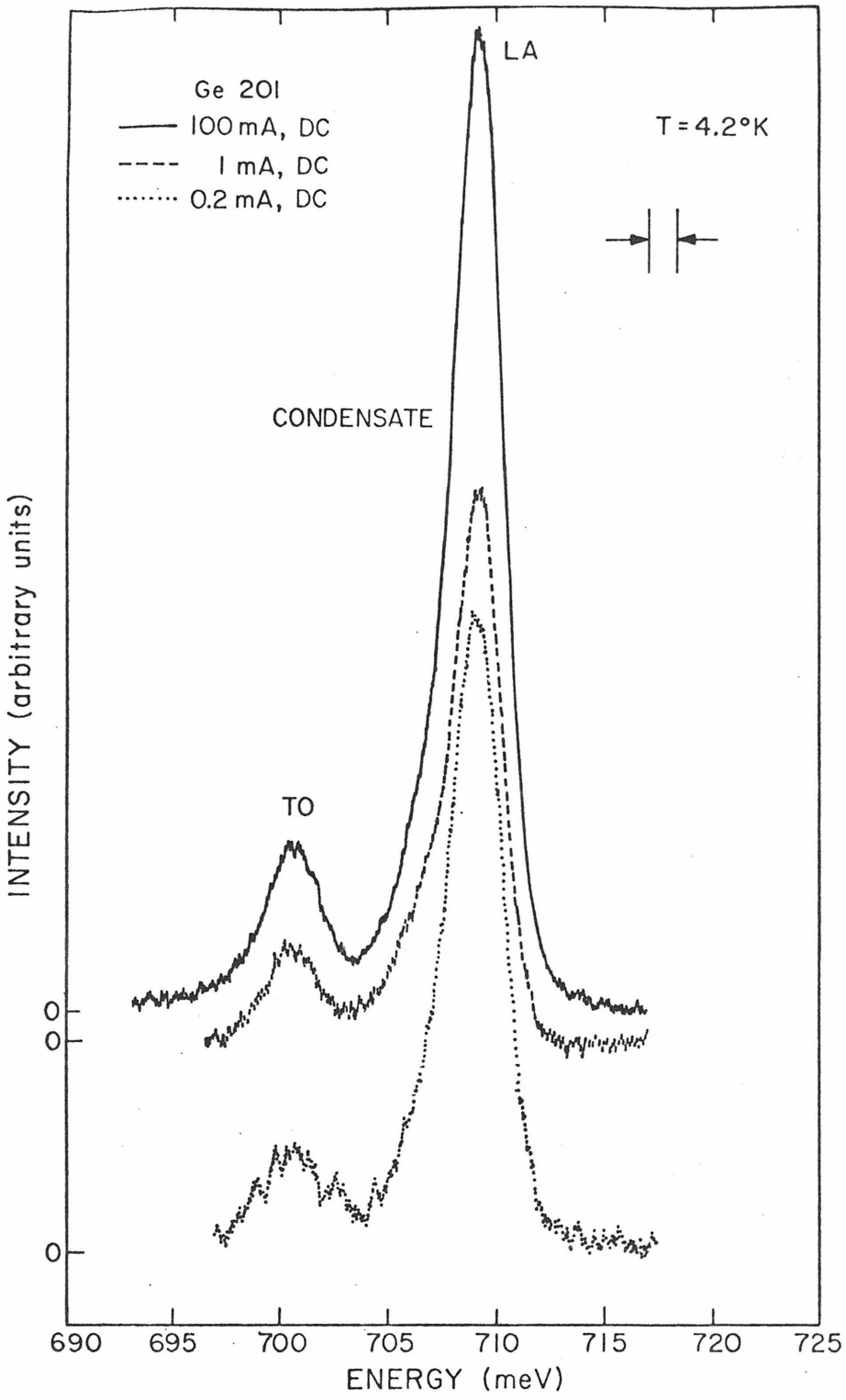
Ge 201
100 mA, DC
1 mA, DC
0.2 mA, DC
T = 4.2°K
LA
CONDENSATE
TO
INTENSITY (arbitrary units)
0
0
0
690
695
700
705
710
715
720
725
ENERGY (meV)

Figure 6

using pulsed currents. The LA- and TO-phonon assisted condensate recombination radiation spectra for three pulsed current levels are shown in Fig. 7. The energy position and linewidth at half maximum are the same as for direct current excitation.

No threshold current for condensate formation was found for any of our double injection diodes within our spectrometer - detector sensitivity limits. This is in contrast to but not in contradiction with the data reported for optical excitation experiments.

2. Temperature Dependence

The recombination radiation spectra from Ge double injection diodes were investigated over a temperature range of 1.5 to 90°K. Figure 8 shows a LA- and TO-phonon assisted condensate recombination radiation spectra from a Ge double injection diode with a pulsed current of 50 mA at 4.2°K and at 2.6°K. No appreciable change in line position or linewidth was noticed as the temperature was lowered below 4.2°K. However, when the temperature was raised above 4.2°K, dramatic changes occurred in the recombination radiation spectra.

Figure 9 shows the LA- and TO-phonon assisted recombination radiation spectra at 4.8°K, 7.2°K, and at 20°K. The line position and linewidth of the condensate recombination radiation lines at 4.8°K is essentially the same as that at 4.2°K. At 7.2°K a significant change in the recombination radiation spectra has occurred. The

Figure 7 LA- and TO-phonon assisted condensate recombination radiation spectra at 4.2 °K for a Ge double injection diode with pulsed currents of 50 mA (4 ms pulse, 6.8% duty cycle, solid line), 100 mA (4 ms pulse, 6.8% duty cycle, dashed line) and 400 mA (4 ms pulse, 36% duty cycle, dotted line). The vertical scales are not the same for the spectra.

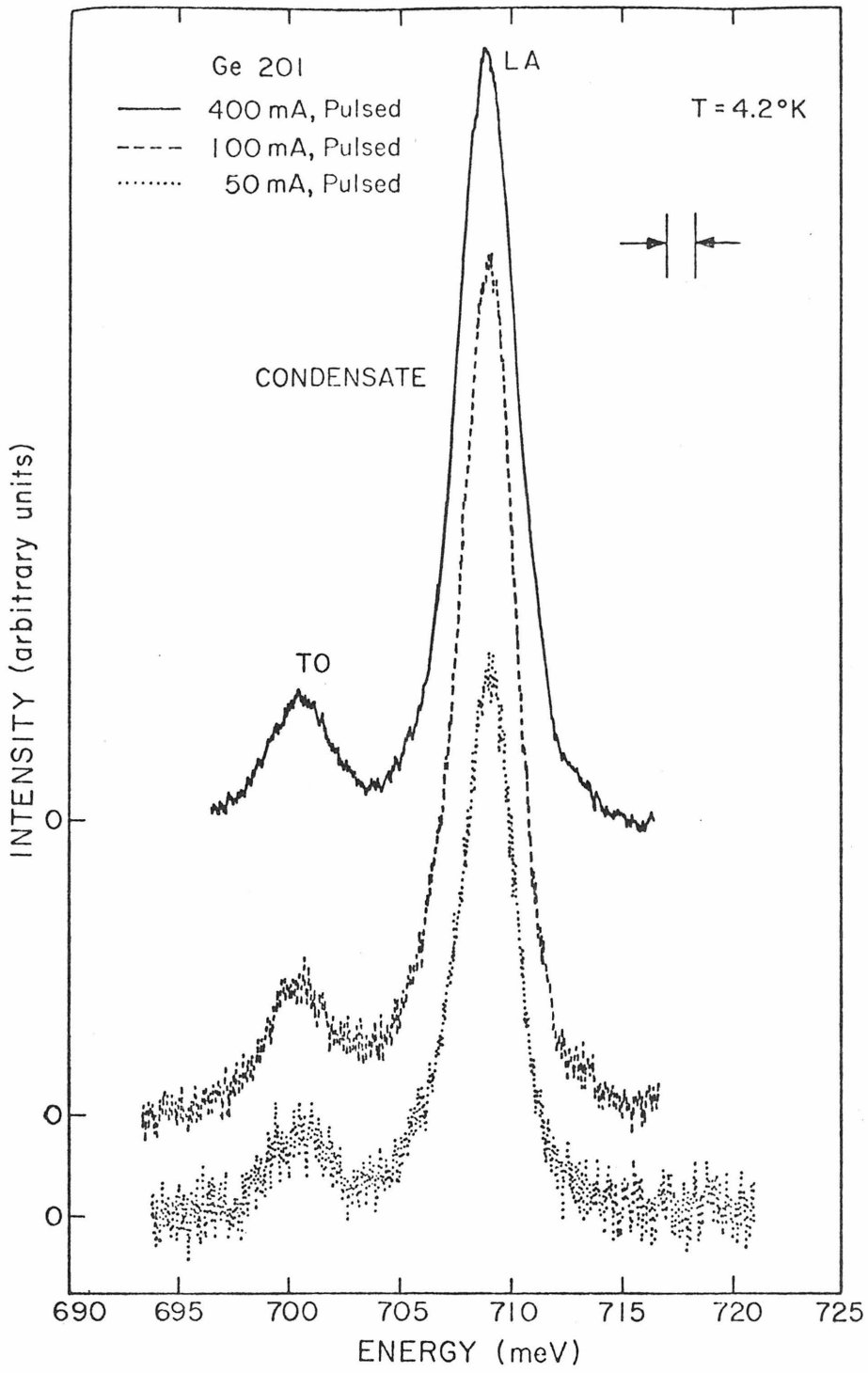
Ge 201
400 mA, Pulsed
100 mA, Pulsed
50 mA, Pulsed
T = 4.2°K
LA
CONDENSATE
TO
INTENSITY (arbitrary units)
690
695
700
705
710
715
720
725
ENERGY (meV)

Figure 7

Figure 8 LA- and TO-phonon assisted condensate recombination radiation spectra of a Ge double injection diode with a pulsed current of 50 mA (4 ms pulse, 6.8% duty cycle) at 4.2°K (dashed line) and of 50 mA (2 ms pulse, 18% duty cycle) at 2.6°K (solid line). The vertical scales are not the same for the spectra.

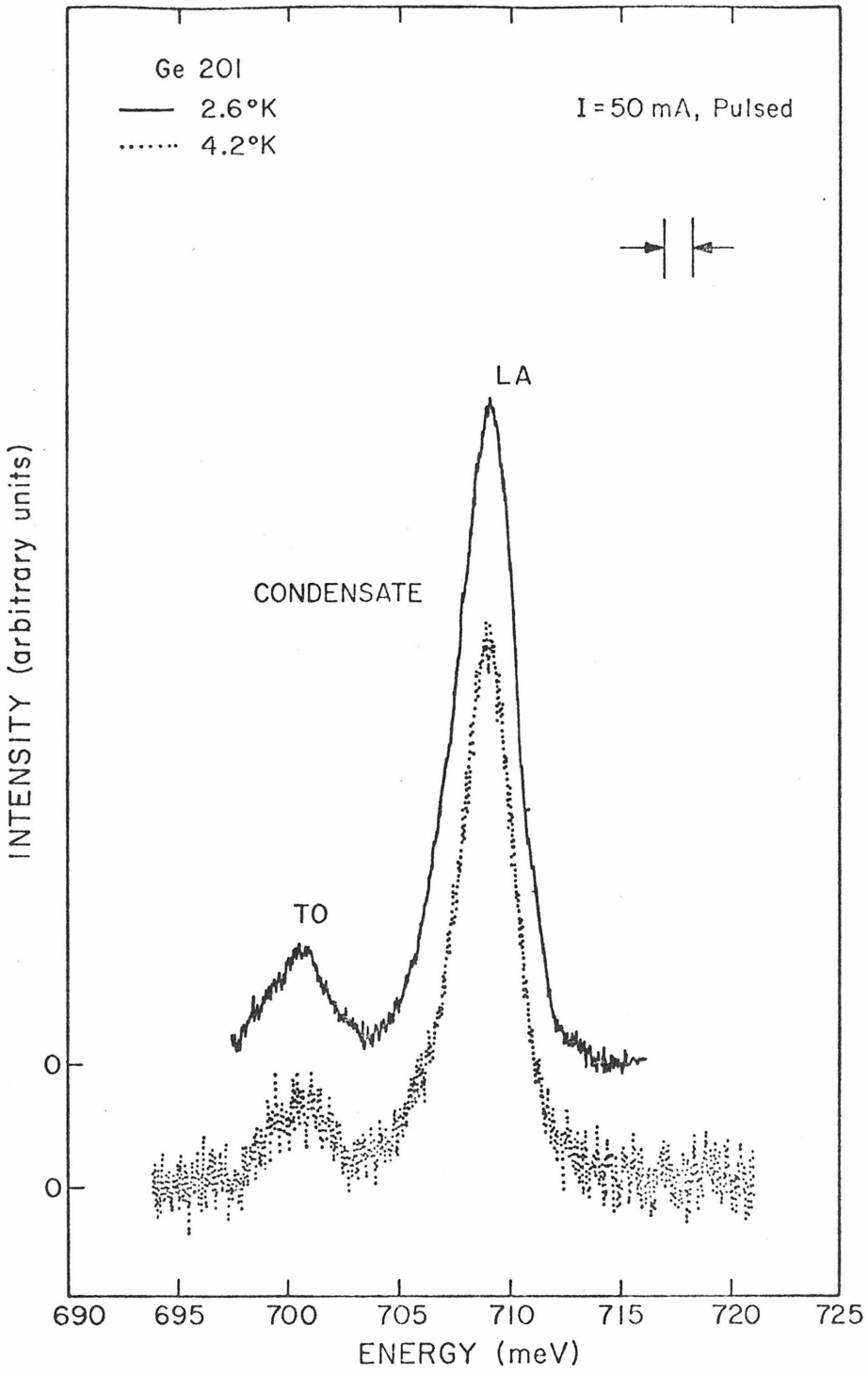
Ge 201
2.6°K
4.2°K
I = 50 mA, Pulsed
LA
CONDENSATE
TO
INTENSITY (arbitrary units)
0
0
690
695
700
705
710
715
720
725
ENERGY (meV)

Figure 8

Figure 9 Phonon assisted recombination radiation spectra for a Ge double injection diode at 20°K (800 mA, 11 ms pulse, 22% duty cycle, solid line), 7.2°K (800 mA, 11 ms pulse, 22% duty cycle, dashed line), and 4.8°K (300 mA, 1 ms pulse, 9% duty cycle, dotted line). The vertical scales are not the same for the spectra.

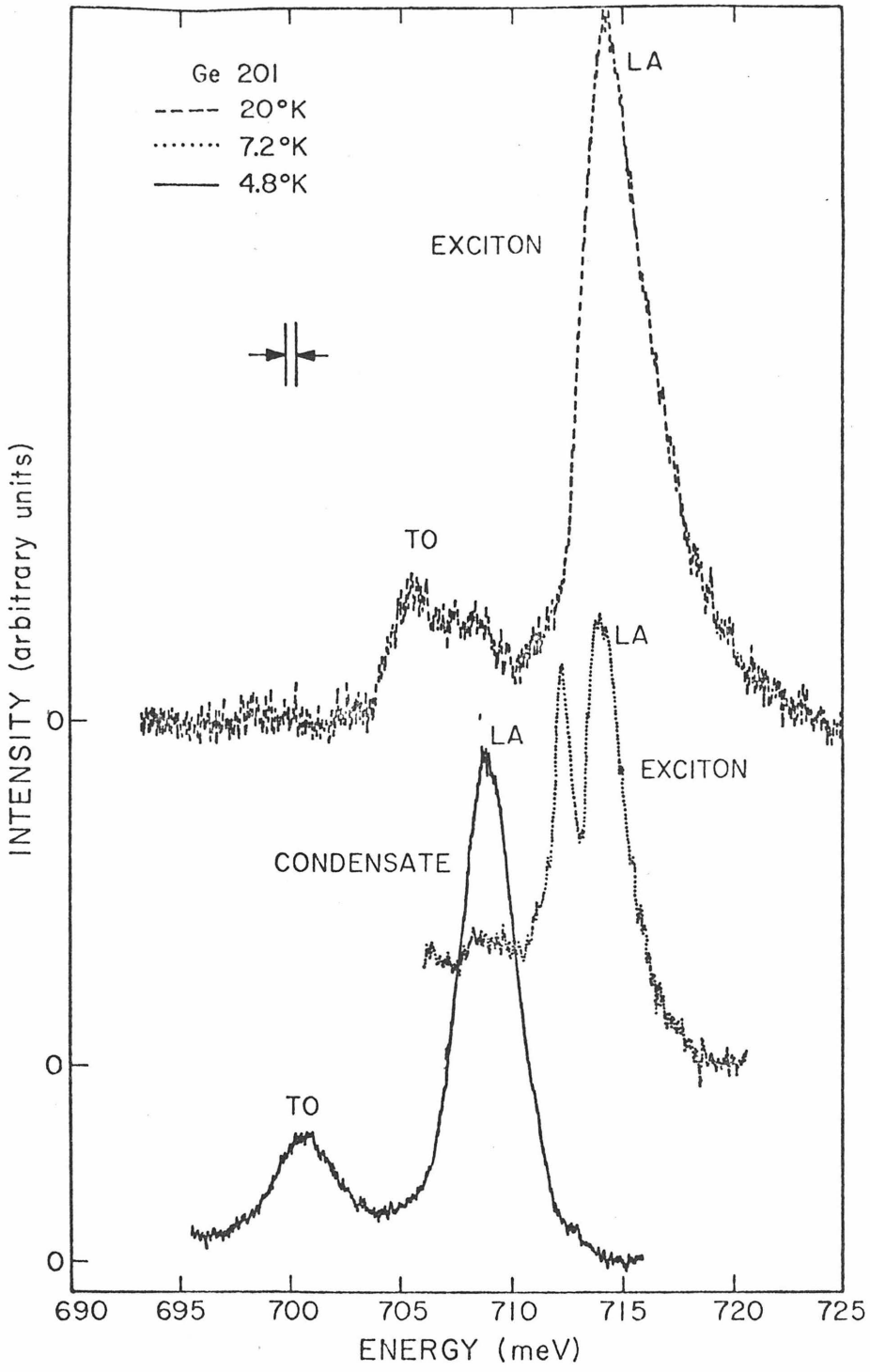
Ge 201
20°K
7.2°K
4.8°K
EXCITON
LA
TO
LA
LA
EXCITON
CONDENSATE
TO
INTENSITY (arbitrary units)
0
0
0
690
695
700
705
710
715
720
725
ENERGY (meV)

Figure 9

LA-phonon assisted line at 709 meV, associated with the condensate, has disappeared and two lines at 712 meV and 714 meV have appeared. The line at 714 meV is the well established LA-phonon assisted exciton recombination radiation line. The other line at 712 meV has been identified [24] as the LA-phonon assisted bound exciton recombination radiation line. Both lines were present at temperature between 7°K to 15°K. The bound exciton line intensity decreased with respect to the exciton line intensity as the temperature was raised. Above 15°K only the exciton line remained. The exciton linewidth decreased with temperature and was always wider than the bound exciton line. The bound exciton linewidth is spectrometer resolution limited.

3. Device Heating Effects

Device temperature can have a significant effect on the recombination radiation spectra of Ge double injection diodes. The possibility of device heating exists even when a constant temperature liquid He bath is used. Heating effects were more apparent in the bar type structures.

At low currents condensate recombination radiation spectra essentially similar to Fig. 8 were obtained for the bar type structures. At higher currents the recombination radiation spectra shown in Fig. 10a were obtained for a bath temperature of 1.9°K and a device current of 260 mA. In this spectrum, the distinct peaks correspond to both exciton and condensate. This result is contrary to that found in the

Figure 10 a) Time integrated recombination spectrum in a bath at 1.9°K with 11 ms injection pulses of 260 mA and 4 V.

b) The time resolved spectrum with the sample in a bath at 2.4°K with 5.6 ms current pulses of 70 mA and 6 V. The solid line (A) gives the spectrum obtained in a gated time interval of 60-160 μs from the beginning of the pulse (see insert). The dotted line (B) gives the spectrum obtained in a gated interval of 160-60 μs from the termination of the current pulse.

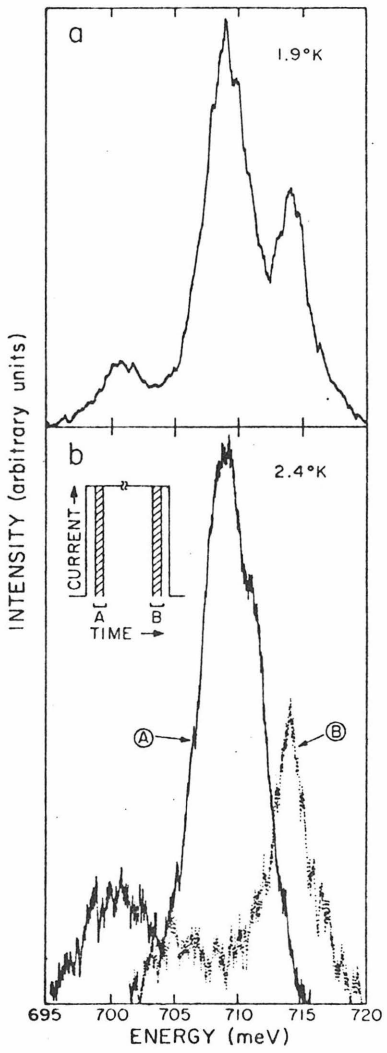
a
1.9°K
b
2.4°K
CURRENT
A
B
TIME
Ⓐ
Ⓑ
INTENSITY (arbitrary units)
695
700
705
710
715
720
ENERGY (meV)

Figure 10

mesa type Ge double injection structures. To investigate variations of such a spectrum during an injection pulse, time resolved spectra were obtained over gated time intervals of 100 μs with the sample at a bath temperature of 2.4°K. The data shown by the solid line, in Fig. 10b, were measured near the beginning of the pulse and exhibit a condensate peak at about 709 meV. The results shown as a dotted line were obtained near the end of the injection pulse and exhibit a free exciton peak at 714 meV. Thus the condensate is present during the initial part of the pulse and excitons during the final part of the pulse. The presence of the excitons and condensate results in the appearance of both peaks in the time integrated spectrum shown in Fig. 10a.

At low power levels, the condensate radiation shows no decay during the current pulse. At higher power levels, the condensate recombination radiation intensity decreases during the current pulse; and the exciton signal appears and increases in intensity. Transient analysis was utilized to show that with increasing power levels the condensate radiation intensity decays giving way to exciton radiation.

Our results show that device heating can have rather a significant influence on the recombination radiation spectrum. The mesa type Ge double injection structures had improved heat dissapation. For this reason, all the data presented in this thesis, except for this part, were obtained on mesa type structures.

4. Dependence of the Recombination Radiation Intensity on Current and Temperature

The temperature and current dependence of the condensate's recombination radiation intensity were investigated in the temperature range of 2 to 4.2°K and in the current range of 15 μA to 1.4 A. The recombination radiation intensity at the 709 meV condensate peak versus direct current at 4.2°K is shown in Fig. 11. The spectrometer had a bandwidth of 1.4 meV. There is a current range where the intensity is linearly proportional to the device current. At higher currents, the intensity versus current is sub-linear; possibly due to device heating. At lower currents the intensity versus current is super-linear. Due to the spectrometer-detector sensitivity it was not possible to determine if this super-linear regime represent a true threshold for condensate formation.

Higher current levels were investigated using pulsed current. Figure 12 shows the recombination radiation intensity of the 709 meV condensate peak from a Ge double injection diode versus pulsed current at 4.2°K. The spectrometer bandwidth is 1.4 meV. The intensity plotted is the recombination radiation intensity in a 50 μs window, 10 μs from the end of a 400 μs current pulse. In the current range from 60 mA to 700 mA the intensity increases linearly with current. At higher currents it begins to decrease. As mentioned before the decrease in the intensity at higher currents is

Figure 11 The recombination radiation intensity of the 709 meV condensate peak for a Ge double injection diode through a spectrometer with bandwidth of 1.4 meV versus direct current at 4.2°K bath temperature.

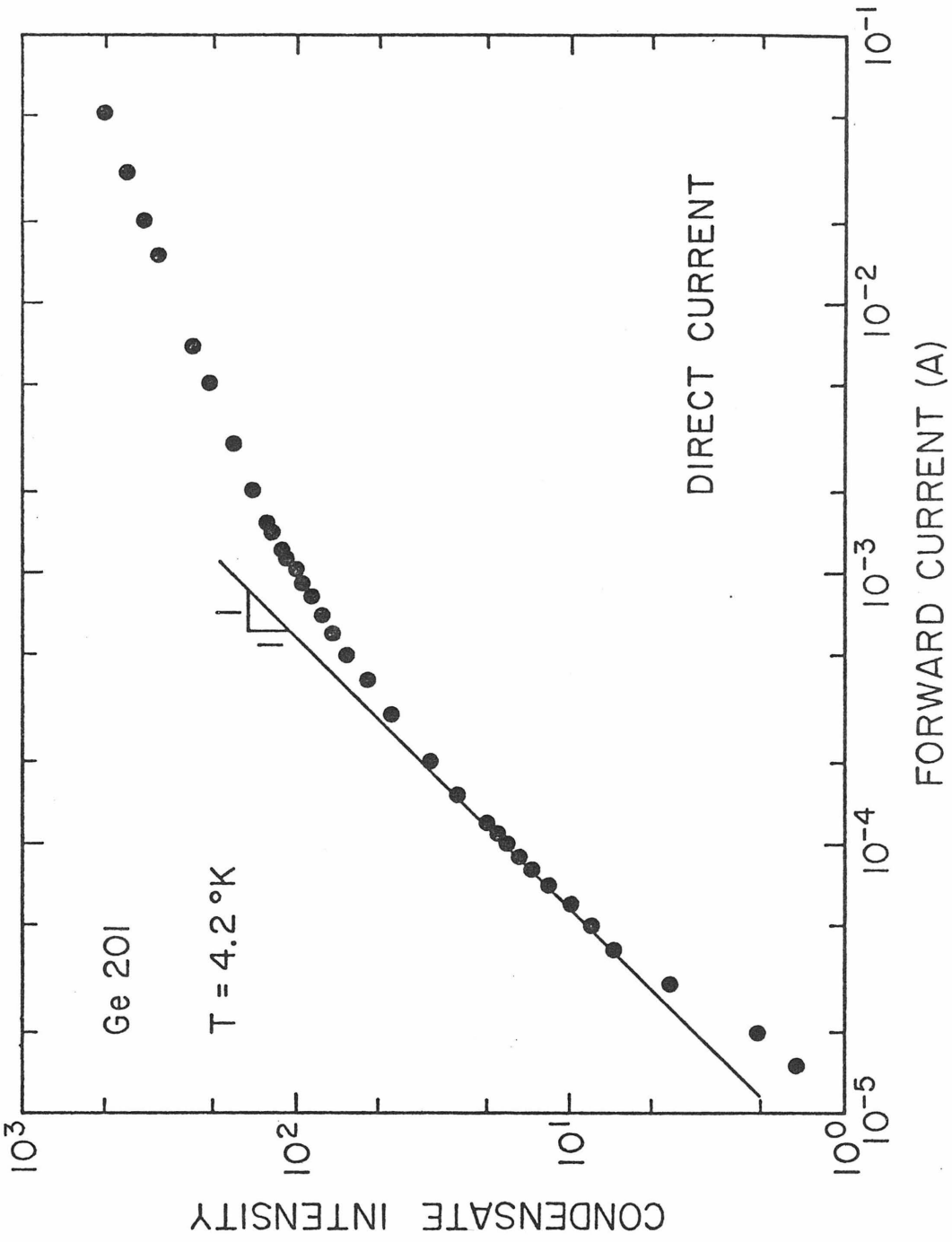
CONDENSATE INTENSITY
FORWARD CURRENT (A)
DIRECT CURRENT
Ge 201
T = 4.2 °K
1
1
10^3
10^2
10^1
10^0
10^{-1}
10^{-2}
10^{-3}
10^{-4}
10^{-5}

Figure 11

Figure 12 The recombination radiation intensity of the 709 meV condensate peak for a Ge double injection diode obtained through the spectrometer having a bandwidth of 1.4 meV versus pulsed currents at 4.2°K. The intensity plotted is the recombination radiation intensity in a 50 μs window, 10 μs from the end of a 400 μs current pulse (0.68% duty cycle). (See insert).

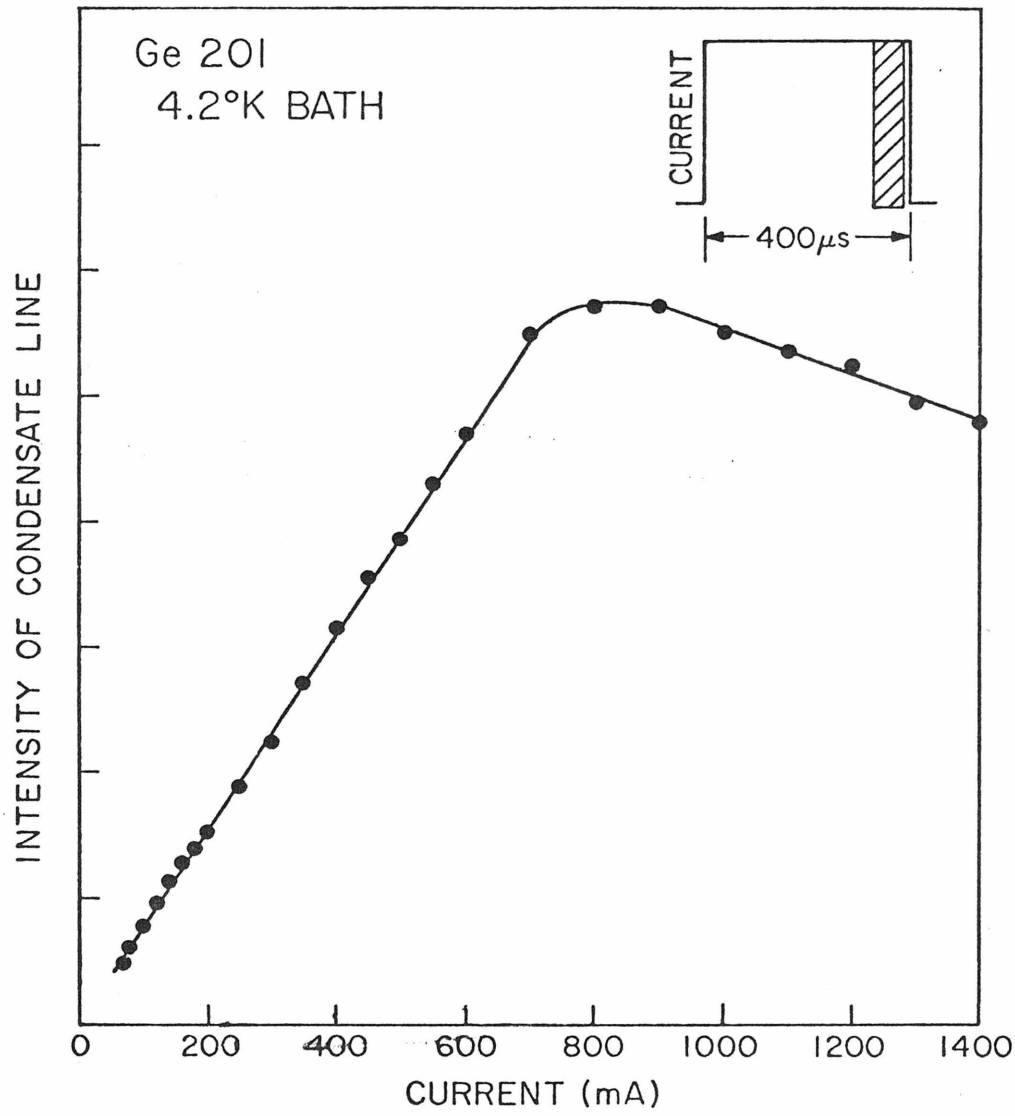
Ge 201
4.2°K BATH
CURRENT
400μs
INTENSITY OF CONDENSATE LINE
0
200
400
600
800
1000
1200
1400
CURRENT (mA)

Figure 12

attributed to device heating.

The temperature dependence of the recombination radiation intensity of the condensate was studied from 2 to 4.2°K. This experiment was performed using a mesa type Ge double injection diode 6 mm^2 by 1.2 mm long. The recombination radiation intensity of the condensate versus pulsed current is shown in Fig. 13 for a bath temperature of 4.2°K (triangles), 3.1°K (squares), 2.7°K (circles) and 2.0°K (dots). These measurements were not made through the spectrometer. Plotted is the recombination radiation intensity at the end of a 100 μs duration current pulse.

At a given temperature the intensity increases with device current. At given current the intensity increases as the temperature is lowered. It can be seen that device temperature has a large effect on recombination radiation intensity from the condensate.

D. Homogeneity of Recombination Radiation from Ge Double Injection Diodes

Surface scans of the recombination radiation indicate that the recombination radiation was emitted predominately from the volume between the n and p contacts for all the temperatures investigated in the range of 1.5 to 90°K. The recombination radiation spectra were the same at the n contact and p contact as they were for the volume between the contacts.

Intensity distribution scans with a lateral resolution of ~ 0.2 mm

Figure 13 The recombination radiation intensity of the condensate from a Ge double injection diode, not through the spectrometer, versus pulsed currents for bath temperatures of 4.2°K (triangles), 3.1°K (squares), 2.7°K (circles) and 2.0°K (dots). The intensity plotted is at the end of a 100 μs duration current pulse (10% duty cycle). The device was of the mesa type with an area of 6 mm^2 and length of 1.2 mm.

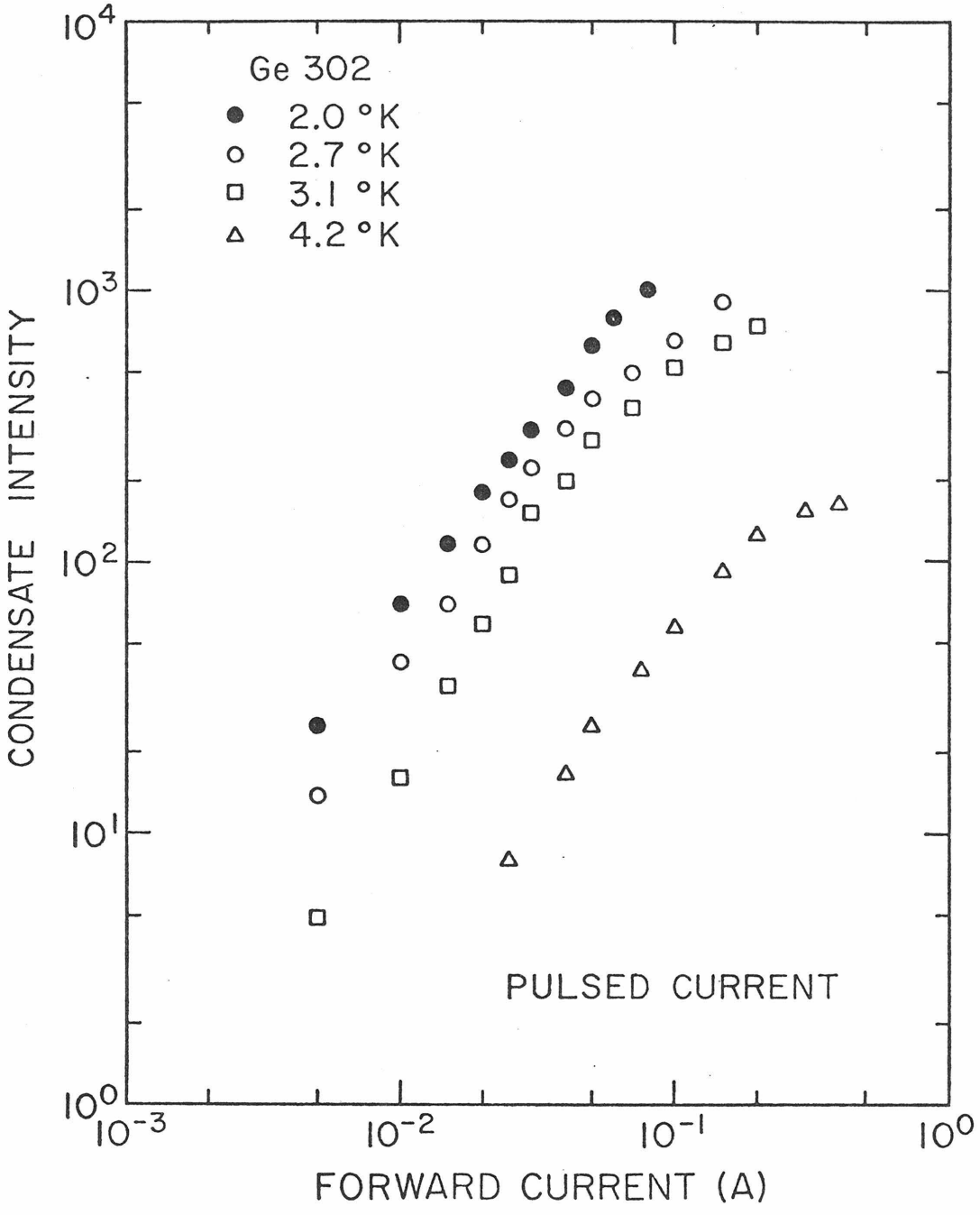
Ge 302
2.0 °K
2.7 °K
3.1 °K
4.2 °K
CONDENSATE INTENSITY
FORWARD CURRENT (A)
PULSED CURRENT
10^4
10^3
10^2
10^1
10^0
10^{-3}
10^{-2}
10^{-1}
10^0

Figure 13

were made between the n and p contacts for a mesa type, 2.4 mm long, Ge double injection diode and are shown in Fig. 14. The scans were made at a pulsed current of 100 mA and at the following temperatures, 4.2, 6.0, 8.7, 14, 31, and 89°K. At 14, 31 and 89°K the recombination radiation intensity scans are similar. Below 14°K, the recombination radiation intensity from the n contact increases relative to the peak. This could be due to the Li donors in the n contact freezing out. At 4.2°K the recombination radiation is emitted almost uniformly from the region between the n and p contacts.

E. Recombination Lifetime of Condensate and Excitons

The recombination radiation lifetimes of both condensate and excitons were measured by applying a constant current pulse to the Ge double injection diode and monitoring the intensity decay after the end of the current pulse. A trace of the recombination radiation intensity from the condensate for a pulsed current of 100 mA is shown in Fig. 15b. Figure 15a shows a trace of the current waveform. Figure 16 shows a current trace and recombination radiation intensity trace at 2°K taken directly from an oscilloscope. The time from the end of the current pulse required for the intensity to decrease to e^{-1} of its maximum value is approximately 40 μs for both temperatures. The logarithm of the recombination radiation intensity from the condensate plotted versus time is shown in Fig. 17. The time dependence of the intensity is exponential with a time constant of 40 μs. This

Figure 14 Recombination radiation intensity scans between the n and p contacts for a mesa type Ge double injection diode at a) 4.2°K, b) 6.0°K, c) 8.7°K, d) 14°K, e) 31°K, and f) 89°K for a pulsed current of 100 mA (1 ms pulsed, 9% duty cycle). The surface was magnified by 3 and imaged onto an infrared detector with a sensitive area of 0.3 mm x 1 mm. The insert shows a schematic diagram of the cross-section of the 2.4 mm long mesa type double injection diode. The intensity scales are not the same for each part of the figure.

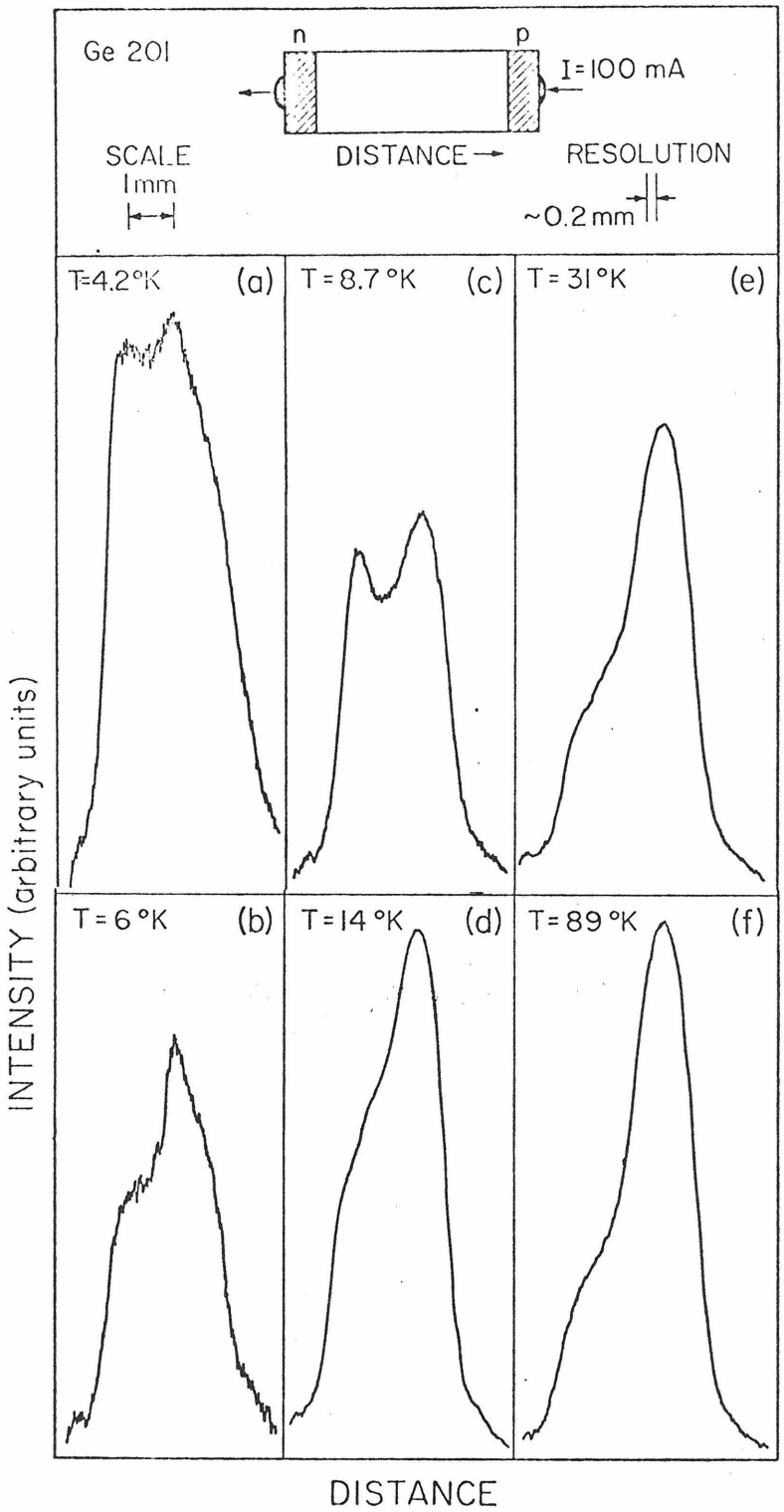
Ge 201
n
p
I=100 mA
SCALE
1mm
DISTANCE
RESOLUTION
~0.2mm
T=4.2°K
(a)
T=8.7°K
(c)
T=31°K
(e)
T=6°K
(b)
T=14°K
(d)
T=89°K
(f)
INTENSITY (arbitrary units)
DISTANCE

Figure 14

Figure 15 A time trace of a) current pulse and b) recombination radiation intensity for a Ge double injection diode with a pulsed current of 100 mA (120 μs pulse, 24% duty cycle) at 3.2°K bath temperature. The mesa type double injection diode is 6 mm^2 by 1.2 mm long.

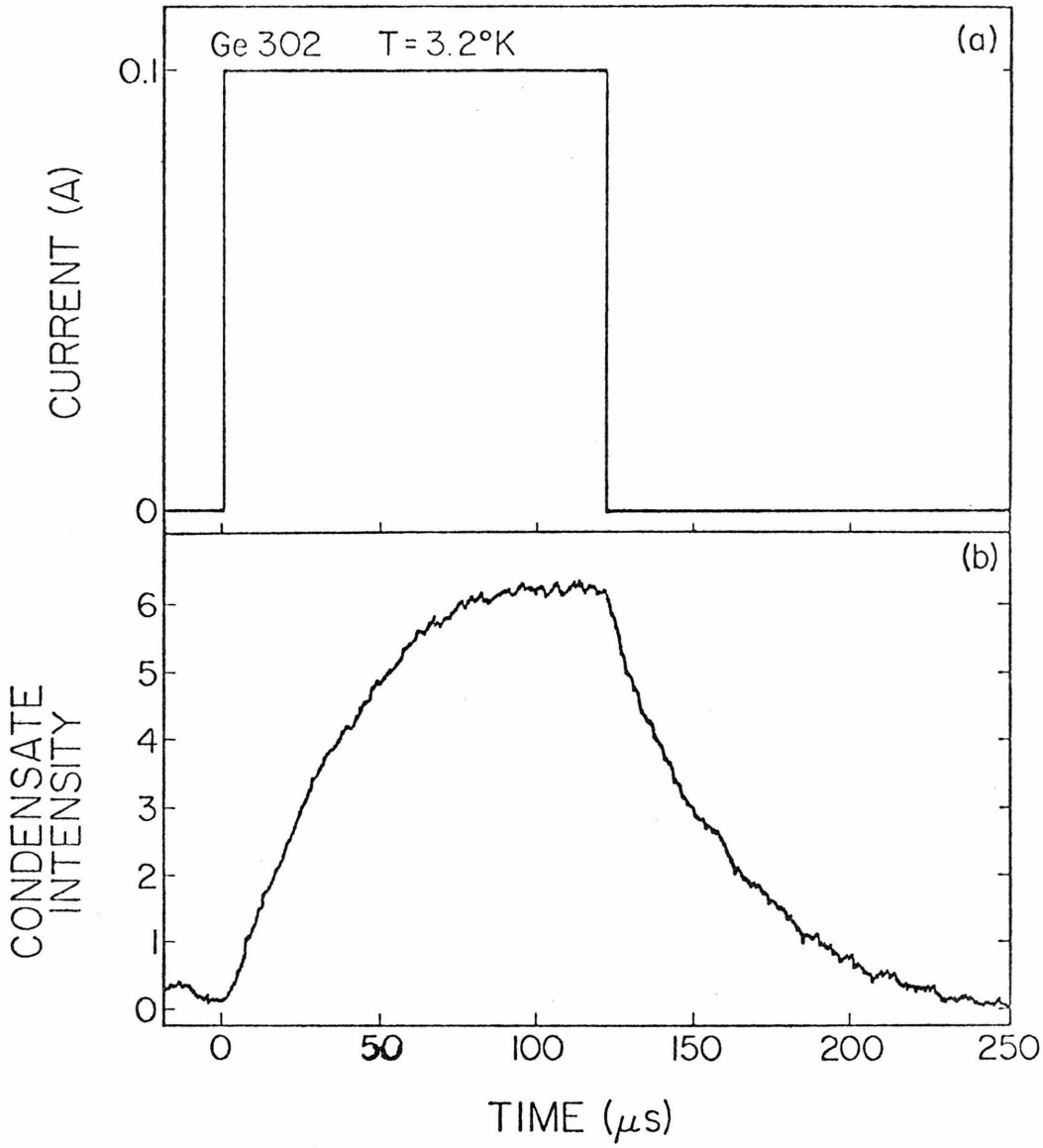
Ge 302 T = 3.2°K
(a)
0.1
0
CURRENT (A)
(b)
6
5
4
3
2
1
0
CONDENSATE INTENSITY
0
50
100
150
200
250
TIME (μs)

Figure 15

gives a condensate lifetime of 40 μs at 3.2°K. Also shown in Fig. 17 is the logarithm of the recombination radiation intensity from the excitons at 20°K following a current pulse. The decay is exponential with a time constant of 6 μs. This gives an exciton lifetime of 6 μs at 20°K. These values are consistent with reported values obtained by optical excitation.[3,5,9]

Figure 16 A time trace of a) current and b) condensate recombination radiation from a Ge double injection diode at 2.0°K bath temperature. The mesa type double injection diode is 6 mm^2 by 1.2 mm long.

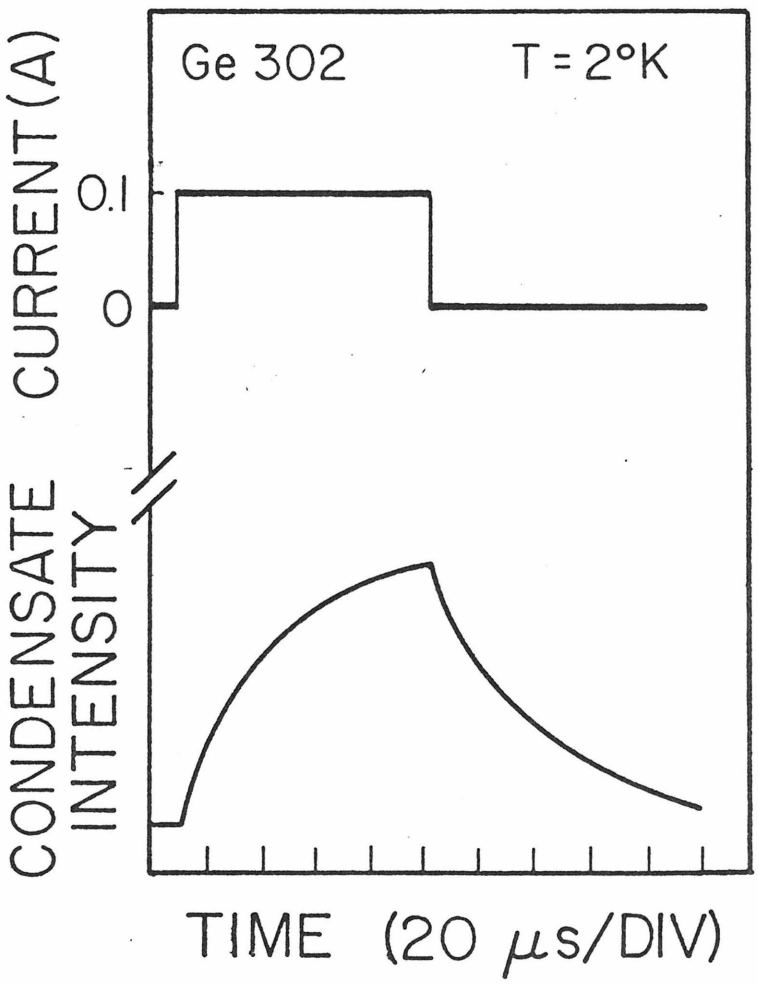

Figure 16

Figure 17 Plot of the log of the recombination radiation intensity following a 100 mA current pulse at 3.2°K (dots) versus time. Also shown is a plot of the log of the recombination radiation intensity following a 500 mA current pulse at 20°K. The condensate lifetime at 3.2°K is 40 μs and the exciton lifetime at 20°K is 6 μs.

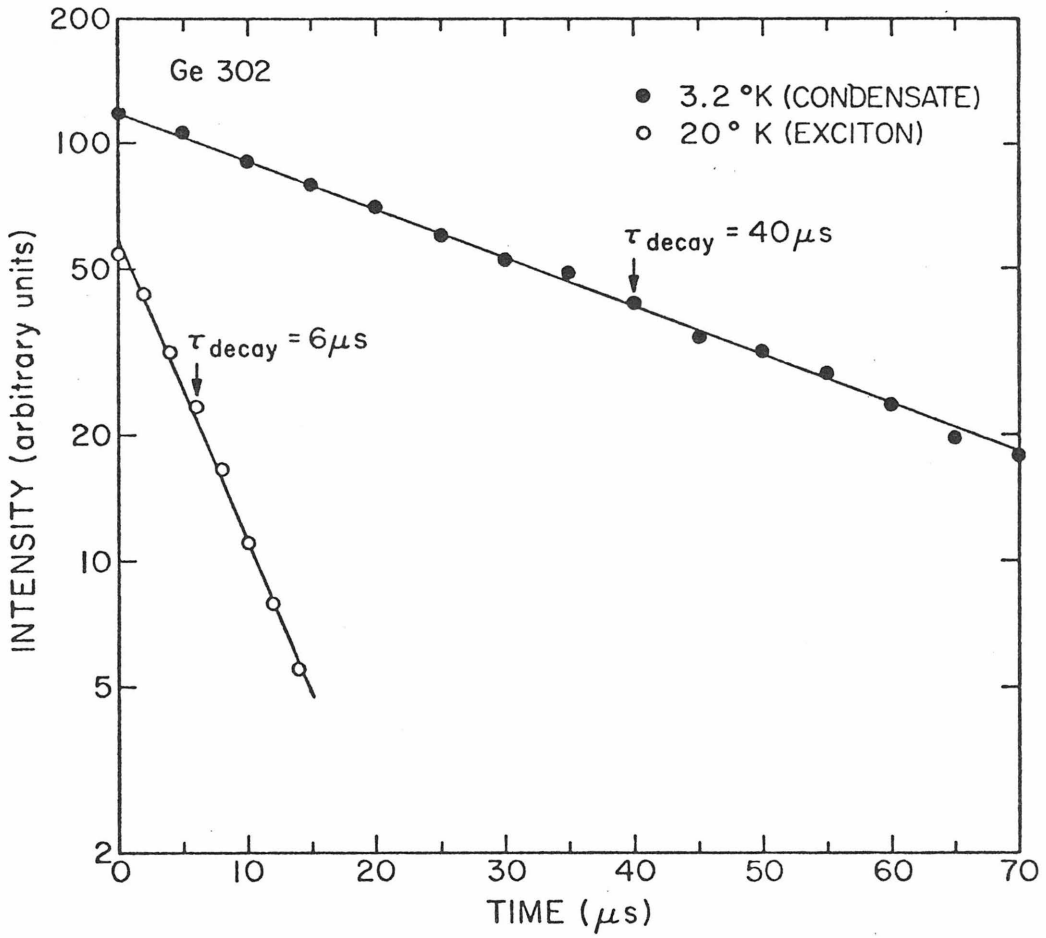
Ge 302
3.2 °K (CONDENSATE)
20 ° K (EXCITON)
τ decay = 40μs
τ decay = 6μs
INTENSITY (arbitrary units)
TIME (μs)
200
100
50
20
10
5
2
0
10
20
30
40
50
60
70

Figure 17

IV. CONCLUSIONS

The condensed phase of electrons and holes does occur in Ge double injection diodes. The condensate was produced by electrical injection of carriers from the contacts. It was present at least up to temperatures of 5°K with either direct or pulsed current excitation.

The LA- and TO-phonon assisted condensate recombination radiation lines occurred at 709 meV and 700 meV respectively. The linewidth at half maximum of the 709 meV line is 3.0 meV. Both line position and linewidth were found to be independent of current and temperature. The recombination radiation lifetime of the condensate is 40 μs.

The LA- and TO-phonon assisted condensate recombination radiation spectra were similar to that obtained in optical injection experiments except for one important difference. We did not observe recombination radiation corresponding to excitons at temperatures below 5°K unless device heating was present. In the optical experiments exciton recombination radiation was always observed down to 2°K. At temperatures above 7°K we observed recombination radiation due to excitions. Above 15°K only the exciton line is observed.

The spatial distribution of the recombination radiation from the condensate indicated that the radiation was emitted almost uniformly from the volume between the contacts. Recombination radiation spectra measured by imaging various parts of the double injection diode onto the spectrometer slits showed that the spectral

nature was the same throughout the double injection diode.

It was found that the intensity of the recombination radiation from the condensate increased with current at constant temperature. At high currents the intensity increased more slowly and eventually began to decrease. This was attributed to device heating. It was also found that the intensity increased as the temperature was lowered at constant current. The intensity depended strongly on temperature. It was not possible to determine a threshold current for condensate formation within the sensitivity of our spectrometer-detector system.

The LA- and TO-phonon assisted exciton recombination radiation lines occured at 714 meV and 706 meV. The line position is approximately independant of temperature. The linewidth at half-maximum is 3.7 meV at 20°K and decreases as the temperature is lowered. The exciton lifetime is 6 μs at 20°K. Only the LA-phonon assisted bound exciton recombination radiation line at 712 meV could be resolved.

The current transport in Ge double injection diodes at low temperatures is not presently understood. The next Section presents speculations on the current transport mechanism.

Electrical injection of carriers into Ge double injection diodes offers a new way to study the collective properties of free electrons and holes, excitons, bound excitons and condensate at liquid He temperatures.

V. SPECULATION ON CURRENT TRANSPORT IN Ge DOUBLE INJECTION DIODES AT LOW TEMPERATURES

I speculate that excitons, bound excitons and condensate play a minor role in the current transport in Ge double injection diodes at low temperatures. Therefore, standard double injection theory is applicable at temperatures down to $2^{o}K$.

This speculation is supported by three observations. First, the intensity of the recombination radiation from the condensate increases continously as the temperature is lowered from 5 to $2^{o}K$ at constant current. This suggests that the volume of the double injection diode is not completely filled with the condensate at temperatures above $2^{o}K$. Second, we do not observe a peak on the recombination radiation spectrum corresponding to the exciton at temperatures below $5^{o}K$. Third, upper bounds on the fraction of the double injection diode filled with the condensate are 0.01 % at $4.2^{o}K$ and 0.2% at $2^{o}K$. These estimates were obtained by measuring the total recombination radiation intensity from the condensate. These three observations above suggest that the device current due to recombination of excitons, bound excitons and condensate is small when compared to the total device current. Therefore it is expected that the majority of the current transport occurs via free carriers.

One way to test the above speculation is to use the absorption of light by electrons and holes to measure the total concentration

of carriers in Ge double injection diodes. Fortunately, a strong light absorption process due to holes is present in Ge at a wavelength of about 3.4 μm.[25,26] This light absorption process has been attributed to inter-valance band hole absorption. The reported cross-section for absorption at a wavelength of 3.4 μm is 1.6×10^{-16} cm^2.[26] This value has been found to be approximately independant of temperature in the range between 77 to 300°K. Since the valance energy bands are not expected to change appreciably below 77°K[27], the light absorption cross-section should not change below 77°K. This light absorption process by holes dominates over free carrier absorption by at least a factor of ten.[25]

A He-Ne laser beam at a wavelength of 3.39 μm can be used to measure the light absorption coefficient due to the injected holes. This can be done by measuring the fractional change in laser beam power due to the current being switched on and off. The average hole concentration can be calculated from the measured absorption coefficient and the absorption cross-section. This in turn will give the average carrier concentration assuming n~p for free carriers, excitons, bound excitons and condensate in the double injection diode.

The above along with known data about excitons, bound excitons, and condensate allows one to put an upper bound on the device current due to recombination of excitons, bound excitons and condensate. The light absorption measurement could be supplemented with voltage probe

measurements across the lightly doped region. One could use this measurement to test agreement with standard double injection theory.[22]

REFERENCES

1. C. Benoît à la Guillaume and O. Parodi, in Proceedings on the on the Fifth International Conference on Semiconductor Physics, Prague, 1960 (Academic, New York, 1961), pg. 426.
2. Ya. Pokrovskii and K. Svistunova, Zh. eksper. teor. Fit. 9, 435 (1969).
3. Ya. Pokrovskii, Phys. Stat. Sol, 11, 385 (1972).
4. Physics Today, 17 (Dec. 1973).
5. C. Benoît à la Guillaume and M. Voos, Phys. Rev. B. 5, 3079 (1972).
6. G. A. Thomas, T. G. Phillips, T. M. Rice, and J. C. Hensel, Phys. Rev. Letters. 31, 386 (1973).
7. V. S. Gagaev, N. A. Penin, N. N. Sibel din and V. A. Tsvetkov, Sov. Phys. Solid State, 15, 2179 (1974).
8. J. C. McGroddy, M. Voos, and O. Christensen, Solid State Comm. 13, 1801 (1973).
9. J. C. Hensel, T. G. Phillips, and T. M. Rice, Phys. Rev. Lett. 30, 227 (1973).
10. V. S. Vavilov, V. A. Zayats and V. N. Murzin, JETP Letts. 10, 192 (1969).
11. G. A. Thomas, T. M. Rice and J. C. Hensel, Phys. Rev. Letts. 23, 219 (1974).
12. L. V. Keldysh, in Proceedings of the Ninth International Converence

of the Physics of Semiconductors, Moscow, 1968 (Nauka, Lenningrad, 1968) p. 1303.

13. M. Combescot and P. Nozieres, J. Phys. C. Proc. Phys. Soc., London 5, 2369 (1972).

14. R. N. Silver, Phy. Rev. B8, 2403 (1973).

15. W. F. Brinkman, T. M. Rice, P. W. Anderson, and S. T. Chui, Phys. Rev. Lett. 28, 961 (1972).

16. W. F. Brinkman and T. M. Rice, Phys. Rev. B7, 1508 (1973).

17. P. Vashishta and S. G. Das and K. S. Singwi, to be published.

18. V. Marrello, T. F. Lee, R. N. Silver, T. C. McGill, and J. W. Mayer, Phys. Rev. Lett. 31, 593 (1973).

19. V. Marrello, R. B. Hammond, R. N. Silver, T. C. McGill, and J. W. Mayer, Phys. Letts. 47, 237 (1974).

20. V. Marrello, T. A. McMath, J. W. Mayer, and I. L. Fowler, Nucl. Inst. and Meth., 108, 93 (1973).

21. J. E. Mercereau (Physics Dept., C. I. T., Pasadena) private communication.

22. R. Baron and J. W. Mayer, Semiconductors and Semimetals, Williardson and Beer, Ed. Academic, New York, 1970) Vol. 6, Chapt. 4.

23. G. Ottaviani, V. Marrello, J. W. Mayer, M-A. Nicolet, and J. M. Caywood, Appl. Phys. Letts., 20, 323 (1972).

24. E. F. Gross, B. N. Novikov and N. S. Sokolov, Solviet Physics - Solid State, 14, 368 (1972).

25. R. A. Smith, Semiconductors, (Cambridge Univ. Press, London, 1959) pg. 216.

26. W. E. Pinson and R. Bray, Phys. Rev. A, 1449 (1964).

27. G. G. Macfarlane, T. P. McLean, J. E. Quarrington and V. Roberts, J. Phys. Chem. Solids, 8, 338 (1959).